IEEE Access
Multidisciplinary ⋮ Rapid Review ⋮ Open Access Journal

Received November 16, 2019, accepted December 2, 2019, date of publication December 12, 2019,
date of current version December 23, 2019.

Digital Object Identifier 10.1109/ACCESS.2019.2959001

Full/Half Duplex Cooperative NOMA Under Imperfect Successive Interference Cancellation and Channel State Estimation Errors

V. ASWATHI, (Student Member, IEEE), AND A. V. BABU, (Senior Member, IEEE)
National Institute of Technology at Calicut, Calicut 673601, India
Corresponding author: V. Aswathi (aswathi481@gmail.com)

ABSTRACT This paper investigates the application of non-orthogonal multiple access (NOMA) in a coordinated direct and relay transmission (CDRT) system, where the base station (BS) directly communicates with the near (i.e., cell-centric) user, while it requires the help of a dedicated full duplex (FD) relay to communicate with the far (i.e., cell-edge) user. For the considered NOMA-FD-CDRT system, we derive closed-form expressions for the outage probabilities and ergodic rates experienced by the downlink users, under the realistic assumptions of imperfect channel state information (I-CSI) and imperfect successive interference cancellation (I-SIC). Expressions for system outage probability and ergodic sum rate are also presented. The links are assumed to experience independent, non-identically distributed Nakagami-*m* fading. The analysis of outage probabilities are carried out for both integer and non-integer values of the fading severity index. Extensive simulation results are described to validate the accuracy of analytical results, and to illustrate the performance gain of the considered system, as compared to NOMA-HD-CDRT system and the orthogonal multiple access (OMA) based CDRT system. Our results show that, both channel estimation error variance and I-SIC factor have significant impact on the performance of the considered NOMA-FD/HD-CDRT system. Further, to ensure fairness in terms of outage, we numerically determine the power allocation coefficient at the BS that provides equal outage performance for both the near and the far users in the presence of I-CSI and I-SIC. Furthermore, we derive closed-form expression for the optimal power allocation (OPA) coefficient at the BS that minimizes the system outage probability of the NOMA-FD/HD-CDRT network under I-CSI. With the help of numerical and simulation investigations, we establish that the proposed OPA significantly reduces the system outage probability, as compared to random (i.e., non-optimal) power allocation at the BS.

INDEX TERMS Channel state information, coordinated direct relay transmission, full/half duplex, non orthogonal multiple access, successive interference cancellation.

I. INTRODUCTION

Recently non-orthogonal multiple access (NOMA) technique has been proposed for improving the efficiency of channel access in the fifth generation (5G) wireless networks. In power domain NOMA, multiple users can coexist and share the same time-frequency resource block by employing power domain multiplexing [1], [2], i.e., the transmitter will use superposition coding for combining multiple user's information signals with distinct power levels; the receiver will use successive interference cancellation (SIC) to decode the message. To enhance the reliability of weak or cell-edge users, cooperative NOMA has been proposed, where either strong users (i.e., users experiencing better channel conditions) or dedicated nodes are configured to act as cooperative relays [3].

In NOMA based coordinated direct and relay transmission (CDRT) system, the base station (BS) directly communicates with the near (i.e., cell-centric) user while it requires the help of a dedicated relay to communicate with the far (i.e., cell-edge) user [4]. Since the BS can transmit the messages intended for the two downlink users in the same time-frequency resource, the spectral efficiency of the resulting NOMA-CDRT system is higher than the conventional orthogonal multiple access (OMA) based CDRT system. Further, in NOMA-CDRT system, the relay node can be

The associate editor coordinating the review of this manuscript and approving it for publication was Antonino Orsino.

operated in two distinct modes: (i) half duplex (HD) or (ii) full duplex (FD). When the relay node operates in HD mode, two distinct time slots (i.e., orthogonal resources) are needed to complete the transmission of message from the BS to the far user via the relay node. In the first time slot, the BS will send the NOMA signal carrying messages for both the near as well as the far user. According to the NOMA principle, the near user will first decode the intended message for the far user and then will apply SIC to decode its own message [3]. Meanwhile, the relay will decode the message corresponding to the far user and will forward the re-encoded message to the far user in the second time slot. Finally, the far user will decode the message at the end of the second time slot.

Operating the relay node in the FD mode enables it to carry out simultaneous reception and transmission [5]. Thus, when the NOMA signal is transmitted by the BS, the relay node implements reception and re-transmission of the re-encoded message in the same time slot. Accordingly, the transmission of the message to the far user can be completed within the duration of one time slot itself (i.e., assuming that the processing delay at the FD relay is negligible). Thus, use of FD relaying further improves the spectral efficiency of the NOMA-CDRT system. However, the resulting NOMA-FD-CDRT system suffers from strong self-interference (SI) at the relay node, which is induced from the relay's transmitter to its receiver section [5]. Even though, the effect of SI can be mitigated by sophisticated interference suppression techniques, the relay node will still be affected by the residual self-interference (RSI), which proportionally grows with the transmit power used at the relay [6]. The focus of the current work is on performance analysis of NOMA-FD/HD-CDRT systems.

A. LITERATURE SURVEY

The performance of HD based cooperative NOMA (i.e., C-NOMA) system has been extensively studied in the literature (e.g., [7]–[11] and references therein). The performance of HD based NOMA-CDRT (i.e., NOMA-HD-CDRT) system has also been studied in the literature [4], [12]–[14]. In [4], the authors have analyzed the outage and ergodic sum rate performance of downlink NOMA-HD-CDRT system. In [12], the authors have considered uplink NOMA in HD-CDRT system, where the ergodic sum capacity has been analyzed under both perfect and imperfect SIC. In [13], the authors have analyzed the outage and ergodic rate performance of the near and the far user in NOMA-HD-CDRT system, where an energy harvesting (EH) relay has been employed to assist the BS for delivering message to the far user. The authors of [14] have considered NOMA in HD-CDRT system with two cell-centric users (CCUs) and a cell-edge user (CEU), which is assisted by a relay. However, operating the relay in HD mode leads to spectral efficiency degradation owing to the requirement for orthogonal resources to carry out reception and transmission at the relay node in C-NOMA system. The current work aims to address this research gap by focusing on the performance analysis of NOMA-FD-CDRT system. Use of in-band FD relaying can improve the spectral efficiency of the CDRT system; however the presence of RSI in FD system reduces the effective signal-to-interference plus noise ratio (SINR) and consequently, there exists a trade-off between the gain in spectral efficiency and performance degradation due to RSI. Accordingly, there is a need to revisit the performance evaluation of NOMA-FD-CDRT system in realistic fading channels.

Recently, NOMA-FD-CDRT system has been considered in [15], where the authors have analyzed the outage and ergodic rate performance assuming perfect channel state information (P-CSI); however due to the existence of the channel estimation errors, such an assumption is too idealistic and does not provide clear insight on the performance of practical networks [16]. The impact of imperfect CSI (I-CSI) on conventional NOMA system has been extensively analyzed, (e.g., [17]–[20] and references therein). The results have shown that I-CSI leads to significant degradation of the performance of NOMA systems. From the detailed literature survey, it has been observed that the analysis of NOMA-FD-CDRT system under the influence of I-CSI has not appeared in the literature so far.

In this paper, we consider a downlink NOMA-FD-CDRT system where user 1 (U_1) is the near user and user 2 (U_2) is the far user. While the BS has direct communication link to U_1, a dedicated FD based relay (R) is used to deliver messages to U_2. According to the NOMA protocol, the strong (near) user has to first decode the symbol intended for the weak (far) user; then use SIC to cancel the signal corresponding to the far user from the received signal, before decoding its own symbol. Now SIC is said to be perfect if the near user has perfect estimate of the symbols corresponding to the far user, which leads to perfect cancellation of the corresponding interference term at the near user. In the presence of imperfect channel estimates, ideal SIC condition cannot be ensured [21]. Thus, we need to consider the residual interference generated at the near user due to imperfect SIC (I-SIC). Accordingly, in this paper, we investigate the impact of I-CSI and I-SIC on the performance of NOMA-FD/HD-CDRT system. Specifically, we focus on the minimum mean square error (MMSE) channel estimation error model reported in [22]. We derive analytical expressions for the outage probabilities experienced by both the near as well as the far users in NOMA-FD/HD-CDRT system under I-CSI and I-SIC. We obtain expression for the system outage probability as well as ergodic sum rate in the presence of I-CSI and I-SIC. Further, we investigate the optimal power allocation (OPA) coefficient at the BS that minimizes the system outage in the presence of I-CSI. To the best of our knowledge, this is the first paper that considers the impact of I-CSI and I-SIC together, on the outage and ergodic rate performance of NOMA-FD/HD-CDRT system, in the presence of RSI.

The performance of FD based C-NOMA system has been investigated extensively in the literature [15], [23]–[33]. In [15], the authors have analyzed the outage and ergodic rate performance of FD C-NOMA system assuming P-CSI/P-SIC. The outage probability, ergodic rate and energy efficiency of FD C-NOMA system has been investigated in [23] under P-CSI/P-SIC. In [24], the authors have analyzed the outage probabilities and ergodic rates of the users in an EH based FD C-NOMA system, assuming P-CSI/P-SIC. In [25], the authors have analyzed the outage and the ergodic sum rate performance of FD C-NOMA system. The OPA factor at the BS to minimize the system outage has been investigated under P-CSI/P-SIC. The outage and ergodic sum rate of NOMA-FD-CDRT system has been analyzed in [26], in Nakagami fading channels under P-CSI/P-SIC. To simplify the analysis, the RSI at the relay node has been modeled as a Gaussian random variable in [26]. Apart from these papers, the performance analysis of FD C-NOMA systems reported in research works [27]–[30] have assumed P-CSI/P-SIC conditions.

The outage performance of FD C-NOMA system has been analyzed in [31] as well, considering Nakagami fading channels under I-SIC; however evaluation of ergodic rates and the ergodic sum rate have been ignored. In [32], the outage and the ergodic sum rate of FD C-NOMA system has been analyzed under I-SIC and I-Q imbalance, in Rayleigh fading channels, ignoring channel estimation errors. The outage performance of FD C-NOMA system has been analyzed in [33] as well under I-SIC; however evaluation of ergodic rates and ergodic sum rate have been ignored. Notice that, none of the above papers consider the impact of I-CSI and I-SIC jointly. Further, the evaluation of system outage probability and the investigation of OPA at the BS to minimize the system outage under I-CSI have been ignored in these papers. Recently, the authors of [34] have investigated the joint effects of residual hardware impairments, channel estimation errors and I-SIC on the outage and ergodic rate performance of EH based C-NOMA system, assuming Nakagami fading channels. The impacts of residual hardware impairments and channel estimation errors on the outage performance of EH based C-NOMA system has been investigated in [35], assuming Weibull fading channels. However, the works in [34], [35] consider HD relaying, which leads to spectral efficiency degradation. In [35], the authors have considered P-SIC in their analysis, while the evaluation of the ergodic rate has been ignored. Moreover, the authors of [34], [35] do not consider the evaluation of the system outage probability of the network and the investigation of OPA that minimizes the system outage probability.

B. MAJOR CONTRIBUTIONS

The major contributions of the paper can be stated as follows:

- We consider NOMA-FD/HD-CDRT system under the realistic assumptions of I-CSI and I-SIC. We consider the channel corresponding to the RSI link at the relay in NOMA-FD-CDRT system to experience Nakagami-m fading.
- We derive closed-form expressions for the outage probabilities experienced by the users and system outage probability in NOMA-FD/HD-CDRT system in the presence of I-CSI and I-SIC, assuming Nakagami-m fading. Approximate closed-form expressions for the ergodic rates of the users are also derived under the influence of I-CSI and I-SIC. We provide expressions for the outage probabilities considering the fact that the fading severity index m can take both integer and non-integer values.
- Extensive evaluations of the impact of I-CSI and I-SIC on the outage and ergodic rate performance of the users are presented. Furthermore, results for the system outage probability and ergodic sum rate are also presented. The performance gain of the considered NOMA-FD-CDRT system has been compared against that of NOMA-HD-CDRT system and the conventional OMA based CDRT system. Analytical results are corroborated by Monte-Carlo based extensive simulation studies.
- It is observed that default selection of NOMA power allocation coefficient at the BS leads to higher outage probability for the near user as compared to the far users. To ensure fairness in terms of outage, we numerically determine the NOMA power allocation coefficient that provides equal outage performance for both the near and the far users in the presence of I-CSI and I-SIC. Analytical expression for the OPA coefficient at the BS that minimizes the system outage probability of NOMA-FD/HD-CDRT network in the presence of I-CSI has been obtained. We evaluate the percentage reduction in system outage probability under the proposed OPA as compared to the random power allocation at the BS. With the help of numerical and simulation investigations, we establish that the system outage improves significantly under the proposed OPA strategy.

The rest of the paper is organized as follows. Section II describes the system model while the derivation of outage probabilities is presented in section III. Section IV describes analytical models for ergodic rates considering I-CSI and I-SIC. Section V considers system outage probability minimization under I-CSI. The results are described in section VI, while section VII describes conclusions.

II. SYSTEM MODEL

We consider a downlink cooperative NOMA-FD-CDRT system as shown in FIGURE 1, where U_1 is the near user and U_2 is the far user. The BS has direct communication link to U_1, while due to heavy shadowing, the direct link between BS and U_2 is absent. Accordingly, the BS employs a dedicated decode-and-forward (DF), full duplex (FD) relay (R) to deliver the messages to U_2. Notice that the message delivery for U_1 happens directly from the BS without the help of the relay node. This model can be applied to a general relay assisted transmission scenario and the related investigations can provide the theoretical foundation for the design of NOMA assisted cooperative networks for future diversified

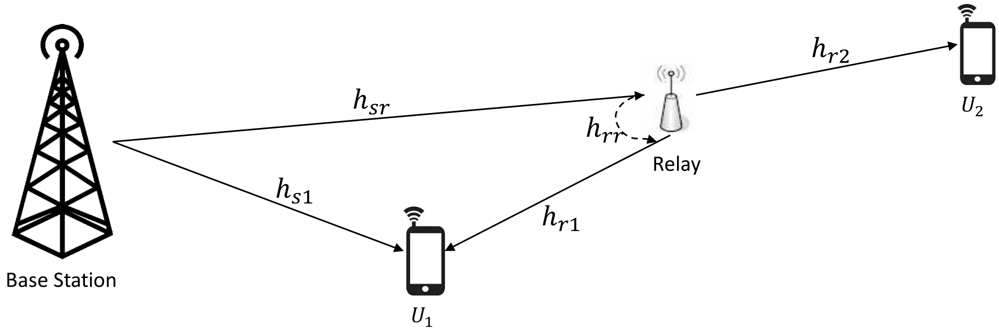

FIGURE 1. **Full duplex based NOMA-CDRT system.**

applications. Let $\{h_{ij}, i \in (s, r), j \in (r, 1, 2)\}$ represent the fading coefficients corresponding to the links between nodes i and j, which are assumed to experience independent, non-identically distributed (i.n.i.d) Nakagami-m fading with shape parameter m_{ij} and mean power $E[|h_{ij}|^2] = \pi_{ij}$. The assumption of Nakagami-m fading model for all the links in the network makes the analysis more general. This is because, Nakagami fading can represent variety of realistic fading scenarios, which include both Rayleigh as well as Rician fading. Under I-CSI, $h_{ij} = \hat{h}_{ij} + \epsilon_{ij}$ [22], where $\hat{h}_{ij}$ denotes the estimated channel coefficient; the probability density function (PDF) of $|\hat{h}_{ij}|$ is assumed as Nakagami-m with shape parameter $|\hat{m}_{ij}|$ and $E[|\hat{h}_{ij}|^2] = \hat{\pi}_{ij}$. Further, ϵ_{ij} is the estimation error, which is assumed as complex Gaussian, i.e., $\epsilon_{ij} \sim CN(0, \sigma_{ij}^2)$ [22]. Assuming that $|\hat{h}_{ij}|^2$ and $|\epsilon_{ij}|^2$ are statistically independent, $E[|\hat{h}_{ij}|^2] = E[|h_{ij}|^2] - E[|\epsilon_{ij}|^2]$. Let $E[|h_{ij}|^2] = \pi_{ij} = (d_{ij}/d_0)^{-n}$ so that $E[|\hat{h}_{ij}|^2] = (d_{ij}/d_0)^{-n} - \sigma_{ij}^2$ where n is the path loss exponent; d_{ij} is the distance of the link connecting nodes i and j; and d_0 is the reference distance.

Notice that $|\hat{h}_{ij}|^2$ have Gamma PDF with shape parameter $\hat{m}_{ij}$ and scale parameter $\hat{\beta}_{ij} = \hat{\pi}_{ij}/\hat{m}_{ij}$. The PDF of $|\hat{h}_{ij}|$ is given by [36]:

$$f_{|\hat{h}_{ij}|}(x) = \left(\frac{\hat{m}_{ij}}{\hat{\pi}_{ij}}\right)^{\hat{m}_{ij}} \frac{(2x)^{\hat{m}_{ij}-1}}{\Gamma(\hat{m}_{ij})} e^{-\frac{\hat{m}_{ij}}{\hat{\pi}_{ij}}x^2} \tag{1}$$

where $\Gamma(.)$ is the gamma function. The PDF of $|\hat{h}_{ij}|^2$ is given by [36]:

$$f_{|\hat{h}_{ij}|^2}(y) = (\hat{\beta}_{ij})^{-\hat{m}_{ij}} \frac{y^{\hat{m}_{ij}-1}}{\Gamma(\hat{m}_{ij})} e^{-\frac{y}{\hat{\beta}_{ij}}} \tag{2}$$

The cumulative distribution function (CDF) of $|\hat{h}_{ij}|^2$ is given by

$$F_{|\hat{h}_{ij}|^2}(y) = \frac{\gamma(\hat{m}_{ij}, \frac{y}{\hat{\beta}_{ij}})}{\Gamma(\hat{m}_{ij})} = \begin{cases} 1 - e^{-y/\hat{\beta}_{ij}} \sum_{k=0}^{\hat{m}_{ij}-1} \frac{(y/\hat{\beta}_{ij})^k}{k!}, \\ \qquad \text{positive integer } \hat{m}_{ij} \\ e^{-\frac{y}{\hat{\beta}_{ij}}} \sum_{n=0}^{\infty} \frac{1}{\Gamma(\hat{m}_{ij}+n+1)} (\frac{y}{\hat{\beta}_{ij}})^{(\hat{m}_{ij}+n)}, \\ \qquad \text{real } \hat{m}_{ij} > \frac{1}{2} \end{cases} \tag{3}$$

where $\gamma(a, b)$ is the incomplete gamma function. Further, frequency flat block fading has been assumed throughout, and all the nodes in the network experience additive white Gaussian noise of equal variance σ^2.

A. SINR CALCULATIONS IN NOMA-FD-CDRT SYSTEM UNDER I-CSI AND I-SIC

The BS applies superposition coding to generate the power domain NOMA signal $x(t)$, which is given by

$$x(t) = \sqrt{P_s a_1} x_1(t) + \sqrt{P_s a_2} x_2(t) \tag{4}$$

where P_s is the total transmit power of the BS; $x_1(t)$ and $x_2(t)$ are the signals for U_1 and U_2 respectively with $E[|x_1(t)|^2] = E[|x_2(t)|^2] = 1$. Here a_1 and a_2 are the power allocation coefficients such that $a_1 + a_2 = 1$ and $a_1 < a_2$. Thus at the BS, U_2 is allocated higher power as compared to U_1. Higher power allocation for the weak user, i.e., U_2 is according to the conventional NOMA principle [3], [4]. When the BS transmits $x(t)$, both R and U_1 will receive the signal in the same time slot. Since R operates in FD mode, it will implement simultaneous reception and transmission, i.e., from the received signal, R decodes the symbol x_2 and forwards it to U_2, after re encoding, in the same time slot. Finally, U_2 decodes x_2 from the received signal. Meanwhile, the near user U_1 will implement SIC to decode x_1 in the same time slot. Assuming that the processing delay at R, U_1 and U_2 are negligible, successful delivery of symbols x_1 and x_2 can be ensured within the duration of the considered time slot itself.

However since R operates in FD mode, it suffers from strong SI, which is the loop back interference induced from its transmitter to the receiver. Since directional antennas can considerably reduce the SI [37], we assume that R employs two directional antennas for implementing simultaneous transmission and reception (STR), while all other nodes in FIGURE 1 use single antenna each. Several other techniques have been proposed for mitigating the SI effects in FD systems [38]–[40]. Inspite of all these developments, researchers have reported that FD nodes suffer from RSI, which is directly proportional to the transmit power used at the FD relay nodes [5], [6]. Further, several experimental studies have reported that the RSI channel can be modeled as a fading channel [40]. Experimental results in [40], [41] have reported that the RSI channel can be modeled as either Rician or Rayleigh. As a generalization, we assume the RSI fading channel coefficient $|h_{rr}|$ to follow Nakagami-m fading with parameters m_{rr} and mean RSI power $E[|h_{rr}|^2] = k_2\pi_{rr}$, where k_2 $(0 \leq k_2 \leq 1)$ denotes the level of SI cancellation, i.e., $k_2 = 0$ implies that RSI is absent in the system.

The received signal at R is given by

$$y_r(t) = (\hat{h}_{sr} + \epsilon_{sr})(\sqrt{P_s a_1}x_1(t) + \sqrt{P_s a_2}x_2(t)) + \sqrt{P_r}h_{rr}x_2(t-\tau) + n_r(t) \quad (5)$$

In (5), the term $\sqrt{P_r}h_{rr}x_2(t-\tau)$ is the RSI, which is independent of the received signal from BS; P_r is the transmit power of R; τ is the processing delay at R and $n_r(t)$ is the AWGN component at R, i.e., $n_r(t) \sim CN(0, \sigma^2)$. When R attempts to decode x_2, the SINR over the BS-R link is given by

$$\Gamma_{r2}^{FD} = \frac{|\hat{h}_{sr}|^2 P_s a_2}{|\hat{h}_{sr}|^2 P_s a_1 + \sigma_{sr}^2 P_s + |h_{rr}|^2 P_r + \sigma^2} = \frac{|\hat{h}_{sr}|^2 \rho_s a_2}{|\hat{h}_{sr}|^2 \rho_s a_1 + |h_{rr}|^2 \rho_r + \sigma_{sr}^2 \rho_s + 1} = \frac{|\hat{h}_{sr}|^2 \rho_s a_2}{|\hat{h}_{sr}|^2 \rho_s a_1 + |h_{rr}|^2 \rho_r + \delta_1} \quad (6)$$

where $\delta_1 = \sigma_{sr}^2\rho_s + 1$, $\rho_s = P_s/\sigma^2$ and $\rho_r = P_r/\sigma^2$. After decoding x_2, R forwards its re-encoded version to U_2 with power P_r. The received signal at U_2 is

$$y_2(t) = (\hat{h}_{r2} + \epsilon_{r2})\sqrt{P_r}x_2(t) + n_2(t) \quad (7)$$

where $n_2(t)$ is the AWGN at U_2. The SINR at U_2 corresponding to the decoding of x_2 is

$$\Gamma_{22}^{FD} = \frac{|\hat{h}_{r2}|^2\rho_r}{\sigma_{r2}^2\rho_r + 1} = \frac{|\hat{h}_{r2}|^2\rho_r}{\delta_2} \quad (8)$$

where $\delta_2 = \sigma_{r2}^2\rho_r + 1$. Meanwhile, the received signal at U_1 is given by

$$y_1(t) = (\hat{h}_{s1} + \epsilon_{s1})[\sqrt{P_s a_1}x_1(t) + \sqrt{P_s a_2}x_2(t)] + \sqrt{P_r}(\hat{h}_{r1} + \epsilon_{r1})x_2(t-\tau) + n_1(t) \quad (9)$$

Notice that $y_1(t)$ includes the received signal from BS and the interference generated at U_1 due to the transmission of the symbol x_2 from R to U_2. From the received signal, U_1 decodes x_2 first and then apply SIC to decode x_1. The SINR corresponding to the decoding of x_2 at U_1 is given by

$$\Gamma_{12}^{FD} = \frac{|\hat{h}_{s1}|^2\rho_s a_2}{|\hat{h}_{s1}|^2\rho_s a_1 + |\hat{h}_{r1}|^2\rho_r + \sigma_{s1}^2\rho_s(a_1 + a_2) + \sigma_{r1}^2\rho_r + 1} = \frac{|\hat{h}_{s1}|^2\rho_s a_2}{|\hat{h}_{s1}|^2\rho_s a_1 + |\hat{h}_{r1}|^2\rho_r + \sigma_{s1}^2\rho_s + \sigma_{r1}^2\rho_r + 1} = \frac{|\hat{h}_{s1}|^2\rho_s a_2}{|\hat{h}_{s1}|^2\rho_s a_1 + |\hat{h}_{r1}|^2\rho_r + \delta_3} \quad (10)$$

where $\delta_3 = \sigma_{s1}^2\rho_s + \sigma_{r1}^2\rho_r + 1$ and $E[|\hat{h}_{r1}|^2] = k_1\pi_{r1}$ with $0 \leq k_1 \leq 1$. When $k_1 = 0$, the residual interference at U_1 due to transmission by U_2 becomes zero. With $0 < k_1 \leq 0$, the interference is non-zero. Notice that U_1 can successfully decode x_2 if and only if $\Gamma_{12}^{FD} > u_2^{FD}$ where u_2^{FD} is the target SINR corresponding to the decoding of symbol x_2.

After decoding x_2, U_1 will try to decode x_1 using SIC. In this case, x_2 must be subtracted from $y_1(t)$ before the decoding of x_1 is carried out. If x_2 is decoded successfully, it can be completely subtracted from the received signal, i.e., SIC will be perfect. Otherwise decoding of x_1 will be carried out in the presence of residual interference due to I-SIC. Thus SINR corresponding to the decoding of x_1 at U_1 in the presence of I-CSI and I-SIC is given by

$$\Gamma_{11}^{FD} = \frac{|\hat{h}_{s1}|^2\rho_s a_1}{\sigma_{s1}^2\rho_s a_1 + |\hat{h}_{s1}|^2\beta\rho_s a_2 + |\hat{h}_{r1}|^2\rho_r + \sigma_{s1}^2\beta\rho_s a_2 + \sigma_{r1}^2\rho_r + 1} = \frac{|\hat{h}_{s1}|^2\rho_s a_1}{|\hat{h}_{s1}|^2\beta\rho_s a_2 + |\hat{h}_{r1}|^2\rho_r + \sigma_{s1}^2\rho_s(a_1 + \beta a_2) + \sigma_{r1}^2\rho_r + 1} = \frac{|\hat{h}_{s1}|^2\rho_s a_1}{\beta a_2\rho_s|\hat{h}_{s1}|^2 + |\hat{h}_{r1}|^2\rho_r + \delta_4} \quad (11)$$

where $\delta_4 = \sigma_{s1}^2\rho_s(a_1 + \beta a_2) + \sigma_{r1}^2\rho_r + 1$ and β is the factor representing the residual interference arising due to I-SIC, where $0 \leq \beta \leq 1$; i.e., $\beta = 0$ means P-SIC and $0 < \beta \leq 1$ implies I-SIC.

B. SINR CALCULATIONS IN NOMA-HD-CDRT SYSTEM UNDER I-CSI AND I-SIC

In NOMA-HD-CDRT system, during time slot 1, the BS transmits the NOMA signal. From the received signal, R decodes the symbol x_2 by treating the signal component corresponding to x_1, as interference. The SINR at R corresponding to the decoding of x_2, Γ_{r2}^{HD} can be written similar to (6), with the exception that the RSI component is absent. Thus Γ_{r2}^{HD} is given by

$$\Gamma_{r2}^{HD} = \frac{|\hat{h}_{sr}|^2\rho_s a_2}{|\hat{h}_{sr}|^2\rho_s a_1 + \delta_1} \quad (12)$$

In the second time slot, R forwards the re-encoded version of x_2 to U_2, where the decoding of x_2 happens. The SINR at U_2 corresponding to the decoding of x_2 is similar to (8) and is given by

$$\Gamma_{22}^{HD} = \frac{|\hat{h}_{r2}|^2\rho_r}{\delta_2} \quad (13)$$

Meanwhile, U_1 receives the NOMA signal in the first time slot itself. Since BS allocates higher power for x_2, the signal component corresponding to x_2 in the received signal at U_1 has higher power. Thus U_1 decodes the far user's symbol x_2 firstly and then use SIC to decode its own symbol x_1. Notice that, since R operates in HD mode, transmission from R happens in the second time slot only. However, decoding of symbols x_2 and x_1 at U_1 happens in the first time slot itself. Thus, unlike the FD case, the decoding of symbols at U_1 is not affected by R's transmission to U_2. Accordingly, the SINR corresponding to the decoding of x_2 and x_1 at U_1 in the NOMA-HD-CDRT system (i.e., Γ_{12}^{HD} and Γ_{11}^{HD} respectively) can be written similar to (10) and (11) respectively, with the exception that the term $|\hat{h}_{r1}|^2\rho_r$ is absent in these expressions. The corresponding equations are given by

$$\Gamma_{12}^{HD} = \frac{|\hat{h}_{s1}|^2\rho_s a_2}{|\hat{h}_{s1}|^2\rho_s a_1 + \delta_3} \tag{14}$$

$$\Gamma_{11}^{HD} = \frac{|\hat{h}_{s1}|^2\rho_s a_1}{\beta a_2\rho_s|\hat{h}_{s1}|^2 + \delta_4} \tag{15}$$

III. ANALYSIS OF OUTAGE PROBABILITY UNDER I-CSI AND I-SIC

In this section, we describe analytical models to find the outage probabilities experienced by U_1 and U_2 as well as the system outage probability under I-CSI and I-SIC. Let r_1 and r_2 be the target rates (expressed in bits per channel use, bpcu) for the successful decoding of symbols x_1 and x_2 respectively. Further, let $u_1^{FD} = 2^{r_1} - 1$ and $u_2^{FD} = 2^{r_2} - 1$ be the corresponding target SINR values.

A. OUTAGE PROBABILITY EXPERIENCED BY U_1 IN NOMA-FD/HD-CDRT NETWORK

As described earlier, U_1 has to decode the symbol x_2 first and then x_1 by using SIC. Thus the probability that U_1 will experience outage in NOMA-FD-CDRT network is given by

$$P_{out,1}^{FD} = 1 - P_r\{\Gamma_{12}^{FD} \geq u_2^{FD}, \Gamma_{11}^{FD} \geq u_1^{FD}\} \tag{16}$$

Case (i): Positive integer values of $\hat{m}_{ij}$

Proposition 1(a): When $u_2^{FD} < \frac{a_2}{a_1}$, $u_1^{FD} < \frac{a_1}{\beta a_2}$, $\beta_1 > \beta_2$, $\alpha_2 > \alpha_1$ and $k_1 \neq 0$, the outage probability of U_1 under the effect of I-CSI and I-SIC is given by (17), as shown at the bottom of this page, where $\alpha_1 = \frac{u_2^{FD}\rho_r}{\rho_s(a_2 - u_2^{FD}a_1)}$, $\beta_1 = \frac{u_2^{FD}\delta_3}{\rho_s(a_2 - u_2^{FD}a_1)}$, $\alpha_2 = \frac{u_1^{FD}\rho_r}{\rho_s(a_1 - \beta u_1^{FD}a_2)}$, $\beta_2 = \frac{u_1^{FD}\delta_4}{\rho_s(a_1 - \beta u_1^{FD}a_2)}$ and ${}^kC_j = \frac{k!}{j!(k-j)!}$. Further, $\gamma(.,.)$ and $\Gamma(.,.)$ are the lower and upper incomplete gamma functions respectively.

Remark 1(a): When $u_2^{FD} < \frac{a_2}{a_1}$, $u_1^{FD} < \frac{a_1}{\beta a_2}$ and $k_1 = 0$, the outage probability of U_1 under the effect of I-CSI and I-SIC is given by

$$P_{out,1}^{FD} = 1 - e^{-\frac{1}{\phi^{FD}\rho_s\hat{\beta}_{s1}}} \sum_{j=0}^{\hat{m}_{s1}-1} \frac{1}{j!}\left(\frac{1}{\phi^{FD}\rho_s\hat{\beta}_{s1}}\right)^j \tag{18}$$

where $\phi^{FD} = \min\left\{\frac{a_2 - u_2^{FD}a_1}{u_2^{FD}\delta_3}, \frac{a_1 - \beta a_2\, u_1^{FD}}{u_1^{FD}\delta_4}\right\}$. Further, when $u_2^{FD} \geq \frac{a_2}{a_1}$ or when $u_1^{FD} \geq \frac{a_1}{\beta a_2}$, $P_{out,1}^{FD}$ becomes unity.

Case (ii): Positive non-integer values of $\hat{m}_{ij}$

Proposition 1(b): When $u_2^{FD} < \frac{a_2}{a_1}$, $u_1^{FD} < \frac{a_1}{\beta a_2}$, $\beta_1 > \beta_2$, $\alpha_2 > \alpha_1$ and $k_1 \neq 0$, the outage probability of U_1 under the effect of I-CSI and I-SIC for positive non-integer values of $\hat{m}_{ij}$ is given by (19), as shown at the bottom of this page.

Remark 1(b): When $u_2^{FD} < \frac{a_2}{a_1}$, $u_1^{FD} < \frac{a_1}{\beta a_2}$ and $k_1 = 0$, the outage probability of U_1 under the effect of I-CSI and

$$\begin{aligned} P_{out,1}^{FD} = 1 - \Bigg[\Bigg[& e^{-\frac{\beta_1}{\hat{\beta}_{s1}}} \sum_{k=0}^{\hat{m}_{s1}-1} \frac{1}{k!}\left(\frac{\alpha_1}{\hat{\beta}_{s1}}\right)^k \frac{(k_1\hat{\beta}_{r1})^{-\hat{m}_{r1}}}{\Gamma(\hat{m}_{r1})} \sum_{j=0}^{k} {}^kC_j\left(\frac{\beta_1}{\alpha_1}\right)^{k-j}\left(\frac{\alpha_1}{\hat{\beta}_{s1}} + \frac{1}{k_1\hat{\beta}_{r1}}\right)^{-j-\hat{m}_{r1}} \\ & \times\gamma\left(j + \hat{m}_{r1}, \left(\frac{\alpha_1}{\hat{\beta}_{s1}} + \frac{1}{k_1\hat{\beta}_{r1}}\right)\left(\frac{\beta_1 - \beta_2}{\alpha_2 - \alpha_1}\right)\right)\Bigg] + \Bigg[e^{-\frac{\beta_2}{\hat{\beta}_{s1}}} \sum_{l=0}^{\hat{m}_{s1}-1} \frac{1}{l!}\left(\frac{\alpha_2}{\hat{\beta}_{s1}}\right)^l \frac{(k_1\hat{\beta}_{r1})^{-\hat{m}_{r1}}}{\Gamma(\hat{m}_{r1})} \\ & \times \sum_{i=0}^{l} {}^lC_i\left(\frac{\beta_2}{\alpha_2}\right)^{l-i}\left(\frac{\alpha_2}{\hat{\beta}_{s1}} + \frac{1}{k_1\hat{\beta}_{r1}}\right)^{-i-\hat{m}_{r1}} \Gamma\left(i + \hat{m}_{r1}, \left(\frac{\alpha_2}{\hat{\beta}_{s1}} + \frac{1}{k_1\hat{\beta}_{r1}}\right)\left(\frac{\beta_1 - \beta_2}{\alpha_2 - \alpha_1}\right)\right)\Bigg]\Bigg] \end{aligned} \tag{17}$$

$$\begin{aligned} P_{out,1}^{FD} = 1 - \Bigg[\Bigg[& \frac{\gamma(\hat{m}_{r1}, (\frac{1}{k_1\hat{\beta}_{r1}})(\frac{\beta_1-\beta_2}{\alpha_2-\alpha_1}))}{\Gamma(\hat{m}_{r1})} - \frac{(k_1\hat{\beta}_{r1})^{-\hat{m}_{r1}}}{\Gamma(\hat{m}_{r1})} \sum_{g=0}^{\infty} \frac{1}{\Gamma(\hat{m}_{s1} + g + 1)}\left(\frac{1}{\hat{\beta}_{s1}}\right)^{\hat{m}_{s1}+g} \\ & \times e^{-\frac{\beta_1}{\hat{\beta}_{s1}}} \sum_{k=0}^{\infty} {}^{\hat{m}_{s1}+g}C_k\left(\frac{\beta_1}{\alpha_1}\right)^k \alpha_1^{\hat{m}_{s1}+g} \frac{\gamma\left(\hat{m}_{s1} + \hat{m}_{r1} + g - k, (\frac{\alpha_1}{\hat{\beta}_{s1}} + \frac{1}{k_1\hat{\beta}_{r1}})(\frac{\beta_1-\beta_2}{\alpha_2-\alpha_1})\right)}{(\frac{\alpha_1}{\hat{\beta}_{s1}} + \frac{1}{k_1\hat{\beta}_{r1}})^{\hat{m}_{s1}+\hat{m}_{r1}+g-k}}\Bigg] \\ & + \Bigg[\frac{\Gamma(\hat{m}_{r1}, (\frac{1}{k_1\hat{\beta}_{r1}})(\frac{\beta_1-\beta_2}{\alpha_2-\alpha_1}))}{\Gamma(\hat{m}_{r1})} - \frac{(k_1\hat{\beta}_{r1})^{-\hat{m}_{r1}}}{\Gamma(\hat{m}_{r1})} \sum_{i=0}^{\infty} \frac{1}{\Gamma(\hat{m}_{s1} + i + 1)}\left(\frac{1}{\hat{\beta}_{s1}}\right)^{\hat{m}_{s1}+i} e^{-\frac{\beta_1}{\hat{\beta}_{s1}}} \\ & \times \sum_{l=0}^{\infty} {}^{\hat{m}_{s1}+i}C_l\left(\frac{\beta_1}{\alpha_1}\right)^l \alpha_1^{\hat{m}_{s1}+i} \frac{\Gamma\left(\hat{m}_{s1} + \hat{m}_{r1} + i - l, (\frac{\alpha_1}{\hat{\beta}_{s1}} + \frac{1}{k_1\hat{\beta}_{r1}})(\frac{\beta_1-\beta_2}{\alpha_2-\alpha_1})\right)}{(\frac{\alpha_1}{\hat{\beta}_{s1}} + \frac{1}{k_1\hat{\beta}_{r1}})^{\hat{m}_{s1}+\hat{m}_{r1}+i-l}}\Bigg]\Bigg] \end{aligned} \tag{19}$$

I-SIC with non-integer values of $\hat{m}_{ij}$ is given by

$$P^{FD}_{out,1} = e^{-\frac{1}{\phi^{FD}\rho_s\hat{\beta}_{s1}}}\left[\sum_{g=0}^{\infty}\frac{1}{\Gamma(\hat{m}_{s1}+g+1)}\times\left(\frac{1}{\phi^{FD}\rho_s\hat{\beta}_{s1}}\right)^{\hat{m}_{s1}+g}\right] \quad (20)$$

Proof: Refer Appendix A.

Corollary 1: To find the outage of U_1 in the equivalent NOMA-HD-CDRT system ($P^{HD}_{out,1}$), we consider the target SINRs for the decoding of x_1 and x_2 as $u^{HD}_1 = 2^{2r_1} - 1$ and $u^{HD}_2 = 2^{2r_2} - 1$. However, as described in section II, successful decoding of symbols at U_1 is not influenced by the RSI present at R and the residual interference caused by $|\hat{h}_{r1}|^2$. Thus $P^{HD}_{out,1}$ can be written similar to $P^{FD}_{out,1}$ given in (18), with necessary modifications:

For positive integer values of $\hat{m}_{ij}$, $P^{HD}_{out,1}$ is given by

$$P^{HD}_{out,1} = 1 - e^{-\frac{1}{\phi^{HD}\rho_s\hat{\beta}_{s1}}}\sum_{j=0}^{\hat{m}_{s1}-1}\frac{1}{j!}\left(\frac{1}{\phi^{HD}\rho_s\hat{\beta}_{s1}}\right)^{j} \quad (21)$$

For positive non-integer values of $\hat{m}_{ij}$, $P^{HD}_{out,1}$ is given by

$$P^{HD}_{out,1} = e^{-\frac{1}{\phi^{HD}\rho_s\hat{\beta}_{s1}}}\left[\sum_{g=0}^{\infty}\frac{1}{\Gamma(\hat{m}_{s1}+g+1)}\left(\frac{1}{\phi^{HD}\rho_s\hat{\beta}_{s1}}\right)^{\hat{m}_{s1}+g}\right] \quad (22)$$

where $\phi^{HD} = \min\left\{\frac{a_2-u^{HD}_2 a_1}{u^{HD}_2\delta_3}, \frac{a_1-\beta a_2 u^{HD}_1}{u^{HD}_1\delta_4}\right\}$; $u^{HD}_2 < \frac{a_2}{a_1}$; $u^{HD}_1 < \frac{a_1}{\beta a_2}$.

B. OUTAGE PROBABILITY EXPERIENCED BY U_2 IN NOMA-FD/HD-CDRT NETWORK

To ensure reliable delivery of symbol x_2 at U_2, it must be decoded successfully at R and U_2. Thus the outage probability experienced by U_2 in NOMA-FD-CDRT system is calculated as follows:

$$P^{FD}_{out,2} = 1 - P_r\{\Gamma^{FD}_{r2} \geq u^{FD}_2; \Gamma^{FD}_{22} \geq u^{FD}_2\} \quad (23)$$

Case (i): Positive integer values of $\hat{m}_{ij}$

Proposition 2(a): When $u^{FD}_2 < \frac{a_2}{a_1}$, the outage probability of U_2 is given by

$$P^{FD}_{out,2} = 1 - \left[e^{-\frac{\delta_1}{\rho_s\psi^{FD}\hat{\beta}_{sr}}}\frac{(k_2\beta_{rr})^{-m_{rr}}}{\Gamma(m_{rr})}\sum_{j=0}^{\hat{m}_{sr}-1}\frac{1}{j!}\times\left(\frac{\rho_r}{\rho_s\psi^{FD}\hat{\beta}_{sr}}\right)^{j}\sum_{l=0}^{j}{}^{j}C_l\left(\frac{\delta_1}{\rho_r}\right)^{j-l}(l+m_{rr}-1)!\times\left(\frac{\rho_r}{\rho_s\psi^{FD}\hat{\beta}_{sr}}+\frac{1}{k_2\beta_{rr}}\right)^{-l-m_{rr}}\times e^{-\frac{u^{FD}_2\delta_2}{\rho_r\hat{\beta}_{r2}}}\sum_{i=0}^{\hat{m}_{r2}-1}\frac{1}{i!}\left(\frac{u^{FD}_2\delta_2}{\rho_r\hat{\beta}_{r2}}\right)^{i}\right] \quad (24)$$

where $\psi^{FD} = \frac{a_2-u^{FD}_2 a_1}{u^{FD}_2}$. Further, $P^{FD}_{out,2}$ becomes unity when $u^{FD}_2 \geq \frac{a_2}{a_1}$.

Case (ii): Positive non-integer values of $\hat{m}_{ij}$

Proposition 2(b): When $u^{FD}_2 < \frac{a_2}{a_1}$, the outage probability of U_2 with positive non-integer values of $\hat{m}_{ij}$ is given by

$$P^{FD}_{out,2} = 1 - \left[\left(1 - \frac{(k_2\hat{\beta}_{rr})^{-\hat{m}_{rr}}}{\Gamma(\hat{m}_{rr})}\sum_{h=0}^{\infty}\frac{1}{\Gamma(\hat{m}_{sr}+h+1)}\times\left(\frac{1}{\rho_s\psi^{FD}\hat{\beta}_{sr}}\right)^{\hat{m}_{sr}+h}e^{-\frac{\delta_1}{\rho_s\psi^{FD}\hat{\beta}_{sr}}}(\rho_r)^{\hat{m}_{sr}+h}\times\sum_{k=0}^{\infty}{}^{\hat{m}_{sr}+h}C_k\left(\frac{\delta_1}{\rho_r}\right)^{k}\frac{\Gamma(\hat{m}_{sr}+\hat{m}_{rr}+h-k)}{\left(\frac{\rho_r}{\rho_s\psi^{FD}\hat{\beta}_{sr}}+\frac{1}{k_2\hat{\beta}_{rr}}\right)^{\hat{m}_{sr}+\hat{m}_{rr}+h-k}}\right)\times\left(1 - e^{-\frac{u^{FD}_2\delta_2}{\rho_r\hat{\beta}_{r2}}}\sum_{g=0}^{\infty}\frac{1}{\Gamma(\hat{m}_{r2}+g+1)}\left(\frac{u^{FD}_2\delta_2}{\rho_r\hat{\beta}_{r2}}\right)^{\hat{m}_{r2}+g}\right)\right] \quad (25)$$

Proof: Refer Appendix B.

Corollary 2: The outage of U_2 in NOMA-HD-CDRT system ($P^{HD}_{out,2}$) can be determined starting from (23) and by following the steps outlined in Appendix B. However, for the HD case, Γ^{HD}_{r2} is given by (12) and Γ^{HD}_{22} is given by (13). Thus the final expression for $P^{HD}_{out,2}$ can be obtained.

For positive integer values of $\hat{m}_{ij}$ $P^{HD}_{out,2}$ is given by

$$P^{HD}_{out,2} = 1 - \left[e^{-\frac{\delta_1}{\rho_s\psi^{HD}\hat{\beta}_{sr}}}\sum_{j=0}^{\hat{m}_{sr}-1}\frac{1}{j!}\left(\frac{\delta_1}{\rho_s\psi^{HD}\hat{\beta}_{sr}}\right)^{j}\times e^{-\frac{u^{HD}_2\delta_2}{\rho_r\hat{\beta}_{r2}}}\sum_{l=0}^{\hat{m}_{r2}-1}\frac{1}{l!}\left(\frac{u^{HD}_2\delta_2}{\rho_r\hat{\beta}_{r2}}\right)^{l}\right] \quad (26)$$

For positive non-integer values of $\hat{m}_{ij}$, $P^{HD}_{out,2}$ is given by

$$P^{HD}_{out,2} = 1 - \left[\left(1 - e^{-\frac{\delta_1}{\psi^{HD}\rho_s\hat{\beta}_{sr}}}\sum_{g=0}^{\infty}\frac{1}{\Gamma(\hat{m}_{sr}+g+1)}\times\left(\frac{\delta_1}{\psi^{HD}\rho_s\hat{\beta}_{sr}}\right)^{\hat{m}_{sr}+g}\right)\times\left(1 - e^{-\frac{u^{HD}_2\delta_2}{\rho_r\hat{\beta}_{r2}}}\times\sum_{h=0}^{\infty}\frac{1}{\Gamma(\hat{m}_{r2}+h+1)}\left(\frac{u^{HD}_2\delta_2}{\rho_r\hat{\beta}_{r2}}\right)^{\hat{m}_{r2}+h}\right)\right] \quad (27)$$

where $\psi^{HD} = \frac{a_2-u^{HD}_2 a_1}{u^{HD}_2}$ and $u^{HD}_2 < \frac{a_2}{a_1}$.

C. SYSTEM OUTAGE PROBABILITY OF NOMA-FD/HD-CDRT NETWORK

Define the system outage probability of the FD-CDRT network as the probability of the event that either any one of the user or both the users suffer outage, i.e.,

$$P^{FD}_{out,sys} = 1 - P_r\{\Gamma^{FD}_{12} \geq u^{FD}_2, \Gamma^{FD}_{11} \geq u^{FD}_1, \Gamma^{FD}_{r2} \geq u^{FD}_2, \Gamma^{FD}_{22} \geq u^{FD}_2\} \quad (28)$$

Case (i): Positive integer values of $\hat{m}_{ij}$

Proposition 3(a): When $u_2^{FD} < \frac{a_2}{a_1}$, $u_1^{FD} < \frac{a_1}{\beta a_2}$, $\beta_1 > \beta_2$, $\alpha_2 > \alpha_1$ and $k_1 \neq 0$, the closed-form expression for $P_{out,sys}^{FD}$ under I-CSI/I-SIC is given by (29), as shown at the bottom of this page.

Remark 2(a): When $u_2^{FD} < \frac{a_2}{a_1}$, $u_1^{FD} < \frac{a_1}{\beta a_2}$ and $k_1 = 0$, the closed-form expression for $P_{out,sys}^{FD}$ under I-CSI/I-SIC is given by:

$$
\begin{aligned}
&P_{out,sys}^{FD}\\
&= 1 - \Bigg[e^{-\frac{1}{\phi^{FD}\rho_s\hat{\beta}_{s1}}} \sum_{j=0}^{\hat{m}_{s1}-1} \frac{1}{j!} \times \left(\frac{1}{\phi^{FD}\rho_s\hat{\beta}_{s1}}\right)^j\\
&\quad \times e^{-\frac{\delta_1}{\rho_s\psi^{FD}\hat{\beta}_{sr}}} \frac{(k_2\beta_{rr})^{-m_{rr}}}{\Gamma(m_{rr})} \sum_{k=0}^{\hat{m}_{sr}-1} \left(\frac{\rho_r}{\rho_s\psi^{FD}\hat{\beta}_{sr}}\right)^k \sum_{l=0}^{k} {}^kC_l\\
&\quad \times \left(\frac{\delta_1}{\rho_r}\right)^{k-l} (l+m_{rr}-1)! \left(\frac{\rho_r}{\rho_s\psi^{FD}\hat{\beta}_{sr}} + \frac{1}{k_2\beta_{rr}}\right)^{-l-m_{rr}}\\
&\quad \times e^{-\frac{u_2^{FD}\delta_2}{\rho_r\hat{\beta}_{r2}}} \sum_{i=0}^{\hat{m}_{r2}-1} \frac{1}{i!} \left(\frac{u_2^{FD}\delta_2}{\rho_r\hat{\beta}_{r2}}\right)^i \Bigg] \qquad (30)
\end{aligned}
$$

where $\phi^{FD} = \min\left\{\frac{a_2 - u_2^{FD}a_1}{u_2^{FD}\delta_3}, \frac{a_1 - \beta a_2\, u_1^{FD}}{u_1^{FD}\delta_4}\right\}$ and $\psi^{FD} = \frac{a_2 - u_2^{FD}a_1}{u_2^{FD}}$. Further, if either $u_2^{FD} \geq \frac{a_2}{a_1}$ or $u_1^{FD} \geq \frac{a_1}{\beta a_2}$, $P_{out,sys}^{FD}$ becomes unity.

Case (ii): Positive non-integer values of $\hat{m}_{ij}$

Proposition 3(b): When $u_2^{FD} < \frac{a_2}{a_1}$, $u_1^{FD} < \frac{a_1}{\beta a_2}$, $\beta_1 > \beta_2$, $\alpha_2 > \alpha_1$ and $k_1 \neq 0$, the closed-form expression for $P_{out,sys}^{FD}$ under I-CSI/I-SIC with positive non-integer values of $\hat{m}_{ij}$ is given by (31), as shown at the bottom of the next page.

Remark 2(b): When $u_2^{FD} < \frac{a_2}{a_1}$, $u_1^{FD} < \frac{a_1}{\beta a_2}$ and $k_1 = 0$, the closed-form expression for $P_{out,sys}^{FD}$ under I-CSI/I-SIC with positive non-integer values of $\hat{m}_{ij}$ is given by

$$
\begin{aligned}
&P_{out,sys}^{FD}\\
&= 1 - \Bigg[\Bigg(\Bigg(1 - e^{-\frac{1}{\phi^{FD}\rho_s\hat{\beta}_{s1}}} \sum_{h=0}^{\infty} \frac{1}{\Gamma(\hat{m}_{s1}+h+1)}\\
&\quad \times \left(\frac{1}{\phi^{FD}\rho_s\hat{\beta}_{s1}}\right)^{\hat{m}_{s1}+h}\Bigg)\Bigg(1 - \frac{(k_2\hat{\beta}_{rr})^{-\hat{m}_{rr}}}{\Gamma(\hat{m}_{rr})}\\
&\quad \times \sum_{g=0}^{\infty} \frac{1}{\Gamma(\hat{m}_{sr}+g+1)} \left(\frac{1}{\rho_s\psi^{FD}\hat{\beta}_{sr}}\right)^{\hat{m}_{sr}+g}\\
&\quad \times e^{-\frac{\delta_1}{\rho_s\psi^{FD}\hat{\beta}_{sr}}} (\rho_r)^{\hat{m}_{sr}+g} \sum_{k=0}^{\infty} {}^{\hat{m}_{sr}+g}C_k \left(\frac{\delta_1}{\rho_r}\right)^k\\
&\quad \times \frac{\Gamma(\hat{m}_{sr}+\hat{m}_{rr}+g-k)}{\left(\frac{\rho_r}{\rho_s\psi^{FD}\hat{\beta}_{sr}} + \frac{1}{k_2\hat{\beta}_{rr}}\right)^{\hat{m}_{sr}+\hat{m}_{rr}+g-k}}\Bigg)\\
&\quad \times \Bigg(1 - e^{-\frac{u_2^{FD}\delta_2}{\rho_r\hat{\beta}_{r2}}} \sum_{i=0}^{\infty} \frac{1}{\Gamma(\hat{m}_{r2}+i+1)} \left(\frac{u_2^{FD}\delta_2}{\rho_r\hat{\beta}_{r2}}\right)^{\hat{m}_{r2}+i}\Bigg)\Bigg] \qquad (32)
\end{aligned}
$$

Proof: Refer Appendix C.

Corollary 3: With HD relaying, Γ_{r2}^{HD} is given by (12); Γ_{22}^{HD}, Γ_{12}^{HD} and Γ_{11}^{HD} are given by (13), (14) and (15) respectively. Thus system outage of NOMA-HD-CDRT ($P_{out,sys}^{HD}$) can be determined by following the steps outlined in Appendix C and for positive integer values of $\hat{m}_{ij}$, $P_{out,sys}^{HD}$ is given by

$$
\begin{aligned}
P_{out,sys}^{HD} &= 1 - \Bigg[e^{-\frac{1}{\phi^{HD}\rho_s\hat{\beta}_{s1}}} \sum_{j=0}^{\hat{m}_{s1}-1} \frac{1}{j!} \left(\frac{1}{\phi^{HD}\rho_s\hat{\beta}_{s1}}\right)^j\\
&\quad \times e^{-\frac{\delta_1}{\rho_s\psi^{HD}\hat{\beta}_{sr}}} \sum_{k=0}^{\hat{m}_{sr}-1} \frac{1}{k!} \left(\frac{\delta_1}{\rho_s\psi^{HD}\hat{\beta}_{sr}}\right)^k\\
&\quad \times e^{-\frac{u_2^{HD}\delta_2}{\rho_r\hat{\beta}_{r2}}} \sum_{i=0}^{\hat{m}_{r2}-1} \frac{1}{i!} \left(\frac{u_2^{FD}\delta_2}{\rho_r\hat{\beta}_{r2}}\right)^i \Bigg] \qquad (33)
\end{aligned}
$$

For positive non-integer values of $\hat{m}_{ij}$, $P_{out,sys}^{HD}$ is given by the following equation:

$$
\begin{aligned}
&P_{out,sys}^{HD}\\
&= 1 - \Bigg[\Bigg(\Bigg(1 - e^{-\frac{1}{\phi^{HD}\rho_s\hat{\beta}_{s1}}} \sum_{g=0}^{\infty} \frac{1}{\Gamma(\hat{m}_{s1}+g+1)}\\
&\quad \times \left(\frac{1}{\phi^{HD}\rho_s\hat{\beta}_{s1}}\right)^{\hat{m}_{s1}+g}\Bigg)\Bigg(1 - e^{-\frac{\delta_1}{\psi^{HD}\rho_s\hat{\beta}_{sr}}}\\
&\quad \times \sum_{h=0}^{\infty} \frac{1}{\Gamma(\hat{m}_{sr}+h+1)} \left(\frac{\delta_1}{\psi^{HD}\rho_s\hat{\beta}_{sr}}\right)^{\hat{m}_{sr}+h}\Bigg)\\
&\quad \times \Bigg(1 - e^{-\frac{u_2^{HD}\delta_2}{\rho_r\hat{\beta}_{r2}}} \sum_{i=0}^{\infty} \frac{1}{\Gamma(\hat{m}_{r2}+i+1)} \left(\frac{u_2^{HD}\delta_2}{\rho_r\hat{\beta}_{r2}}\right)^{\hat{m}_{r2}+i}\Bigg)\Bigg] \qquad (34)
\end{aligned}
$$

$$
\begin{aligned}
P_{out,sys}^{FD} &= 1 - \Bigg[\Bigg[\Bigg[e^{-\frac{\beta_1}{\hat{\beta}_{s1}}} \sum_{k=0}^{\hat{m}_{s1}-1} \frac{1}{k!} \left(\frac{\alpha_1}{\hat{\beta}_{s1}}\right)^k \frac{(k_1\hat{\beta}_{r1})^{-\hat{m}_{r1}}}{\Gamma(\hat{m}_{r1})} \sum_{j=0}^{k} {}^kC_j \left(\frac{\beta_1}{\alpha_1}\right)^{k-j} \left(\frac{\alpha_1}{\hat{\beta}_{s1}} + \frac{1}{k_1\hat{\beta}_{r1}}\right)^{-j-\hat{m}_{r1}}\\
&\quad \times \gamma\left(j+\hat{m}_{r1}, \left(\frac{\alpha_1}{\hat{\beta}_{s1}} + \frac{1}{k_1\hat{\beta}_{r1}}\right)\left(\frac{\beta_1-\beta_2}{\alpha_2-\alpha_1}\right)\right)\Bigg] + \Bigg[e^{-\frac{\beta_2}{\hat{\beta}_{s1}}} \sum_{l=0}^{\hat{m}_{s1}-1} \frac{1}{l!} \left(\frac{\alpha_2}{\hat{\beta}_{s1}}\right)^l \frac{(k_1\hat{\beta}_{r1})^{-\hat{m}_{r1}}}{\Gamma(\hat{m}_{r1})} \sum_{p=0}^{l} {}^lC_p \left(\frac{\beta_2}{\alpha_2}\right)^{l-p}\\
&\quad \times \left(\frac{\alpha_2}{\hat{\beta}_{s1}} + \frac{1}{k_1\hat{\beta}_{r1}}\right)^{-p-\hat{m}_{r1}} \Gamma\left(p+\hat{m}_{r1}, \left(\frac{\alpha_2}{\hat{\beta}_{s1}} + \frac{1}{k_1\hat{\beta}_{r1}}\right)\left(\frac{\beta_1-\beta_2}{\alpha_2-\alpha_1}\right)\right)\Bigg]\Bigg] e^{-\frac{\delta_1}{\rho_s\psi^{FD}\hat{\beta}_{sr}}} \frac{(k_2\beta_{rr})^{-m_{rr}}}{\Gamma(m_{rr})} \sum_{x=0}^{\hat{m}_{sr}-1} \left(\frac{\rho_r}{\rho_s\psi^{FD}\hat{\beta}_{sr}}\right)^x\\
&\quad \times \sum_{y=0}^{x} {}^xC_y \left(\frac{\delta_1}{\rho_r}\right)^{x-y} (y+m_{rr}-1)! \left(\frac{\rho_r}{\rho_s\psi^{FD}\hat{\beta}_{sr}} + \frac{1}{k_2\beta_{rr}}\right)^{-y-m_{rr}} e^{-\frac{u_2^{FD}\delta_2}{\rho_r\hat{\beta}_{r2}}} \sum_{i=0}^{\hat{m}_{r2}-1} \frac{1}{i!} \left(\frac{u_2^{FD}\delta_2}{\rho_r\hat{\beta}_{r2}}\right)^i \Bigg] \qquad (29)
\end{aligned}
$$

where $\phi^{HD} = \min\left\{\frac{a_2-u_2^{HD}a_1}{u_2^{HD}\delta_3}, \frac{a_1-\beta a_2\, u_1^{HD}}{u_1^{HD}\delta_4}\right\}$, $\psi^{HD} = \frac{a_2-u_2^{HD}a_1}{u_2^{HD}}$, $u_2^{HD} < \frac{a_2}{a_1}$ and $u_1^{HD} < \frac{a_1}{\beta a_2}$.

IV. ANALYSIS OF ERGODIC RATE

Here we present analytical models to evaluate ergodic rates over the BS-U_1 and BS-U_2 links.

A. ERGODIC RATE OF U_1 IN NOMA-FD/HD-CDRT NETWORK

The ergodic rate achieved by U_1 in NOMA-FD-CDRT network ($E[R_1^{FD}]$) is determined as follows:

$$\begin{aligned} E[R_1^{FD}] &= E[log_2(1+\Gamma_{11}^{FD})] \\ &= \int_0^\infty log_2(1+x) f_{\Gamma_{11}^{FD}}(x)dx \\ &= \frac{1}{ln2}\int_0^\infty \frac{1-F_{\Gamma_{11}^{FD}}(x)}{1+x}dx \end{aligned} \tag{35}$$

where $f_{\Gamma_{11}^{FD}}(x)$ and $F_{\Gamma_{11}^{FD}}(x)$ respectively are the PDF and CDF of Γ_{11}^{FD}.

Proposition 4: When $k_1 \neq 0$, an approximate closed-form expression for $E[R_1^{FD}]$ in the presence of I-CSI/I-SIC obtained by using Gaussian-Chebyshev quadrature is given by:

$$\begin{aligned} E[R_1^{FD}] \cong \frac{\pi}{Nln2}\frac{(k_1\hat{\beta}_{r1})^{-\hat{m}_{r1}}}{\Gamma(\hat{m}_{r1})}\sum_{k=0}^{\hat{m}_{s1}-1}\frac{1}{k!}\sum_{i=0}^{k} {}^kC_i\left(\frac{\delta_4}{\rho_r}\right)^{k-i} \\ \times (i+\hat{m}_{r1}-1)!\sum_{n=1}^{N}\frac{a_n p_n}{b_n}e^{-c_n} \end{aligned} \tag{36}$$

where

$$\begin{aligned} a_n &= \left(\frac{(\phi_n+1)\rho_r}{a_2\beta\rho_s(1-\phi_n)\hat{\beta_{s1}}}\right)^k\sqrt{(1-\phi_n^2)}, \\ b_n &= 2\, a_2\beta + a_1(\phi_n+1), \\ c_n &= \left(\frac{(\phi_n+1)\delta_4}{a_2\beta\rho_s(1-\phi_n)\hat{\beta_{s1}}}\right), \\ p_n &= \left(\frac{(\phi_n+1)\rho_r}{a_2\beta\rho_s(1-\phi_n)\hat{\beta_{s1}}}+\frac{1}{k_1\hat{\beta}_{r1}}\right)^{-k-\hat{m}_{r1}}, \\ \phi_n &= cos(\frac{(2n-1)\pi}{2N}) \end{aligned}$$

and N is the complexity-accuracy trade-off parameter.

Remark 3: When $k_1 = 0$, an approximate closed-form expression for $E[R_1^{FD}]$ in the presence of I-CSI/I-SIC obtained by using Gaussian-Chebyshev quadrature is given by:

$$E[R_1^{FD}] \cong \frac{\pi}{Nln2}\sum_{j=0}^{\hat{m}_{s1}-1}\frac{1}{j!}\sum_{n=1}^{N}\frac{o_n}{b_n}e^{-c_n} \tag{37}$$

where $o_n = \left(\frac{(\phi_n+1)\delta_4}{a_2\beta\rho_s(1-\phi_n)\hat{\beta_{s1}}}\right)^k\sqrt{(1-\phi_n^2)}$. Further b_n, c_n, ϕ_n and N are defined as above.

Proof: Refer Appendix D.

Corollary 4: With HD relaying, Γ_{11}^{HD} is given by (15). Thus ergodic rate of U_1 in NOMA-HD-CDRT system ($E[R_1^{HD}]$) under I-CSI/I-SIC is given by:

$$E[R_1^{HD}] \cong \frac{\pi}{N(2ln2)}\sum_{j=0}^{\hat{m}_{s1}-1}\frac{1}{j!}\sum_{n=1}^{N}\frac{o_n}{b_n}e^{-c_n} \tag{38}$$

B. ERGODIC RATE OF U_2 IN NOMA-FD/HD-CDRT NETWORK

The ergodic rate of U_2 ($E[R_1^{HD}]$) in NOMA-FD/HD-CDRT system is determined as follows:

$$\begin{aligned} E[R_2^{FD}] &= E[log_2(1+min\{\Gamma_{12}^{FD},\Gamma_{r2}^{FD},\Gamma_{22}^{FD}\})] \\ &= E[log_2(1+Y)] \\ &= \frac{1}{ln2}\int_0^\infty\frac{1-F_Y(y)}{1+y}dy \end{aligned} \tag{39}$$

where $F_Y(y)$ is the CDF of $Y = min\{\Gamma_{12}^{FD},\Gamma_{r2}^{FD},\Gamma_{22}^{FD}\}$.

$$\begin{aligned} P_{out,sys}^{FD} = 1 - \Bigg[\Bigg[\Bigg[\Bigg(&\frac{\gamma(\hat{m}_{r1},(\frac{1}{k_1\hat{\beta}_{r1}})(\frac{\beta_1-\beta_2}{\alpha_2-\alpha_1}))}{\Gamma(\hat{m}_{r1})} - \frac{(k_1\hat{\beta_{r1}})^{-\hat{m}_{r1}}}{\Gamma(\hat{m}_{r1})}\sum_{g=0}^{\infty}\frac{1}{\Gamma(\hat{m}_{s1}+g+1)}\left(\frac{1}{\hat{\beta}_{s1}}\right)^{\hat{m}_{s1}+g}e^{-\frac{\beta_1}{\hat{\beta}_{s1}}} \\ &\times\sum_{k=0}^{\infty}{}^{\hat{m}_{s1}+g}C_k\left(\frac{\beta_1}{\alpha_1}\right)^k\alpha_1^{\hat{m}_{s1}+g}\frac{\gamma\left(\hat{m}_{s1}+\hat{m}_{r1}+g-k,(\frac{\alpha_1}{\hat{\beta}_{s1}}+\frac{1}{k_1\hat{\beta}_{r1}})(\frac{\beta_1-\beta_2}{\alpha_2-\alpha_1})\right)}{(\frac{\alpha_1}{\hat{\beta}_{s1}}+\frac{1}{k_1\hat{\beta}_{r1}})^{\hat{m}_{s1}+\hat{m}_{r1}+g-k}}\Bigg)\Bigg] \\ &+\Bigg[\Bigg(\frac{\Gamma(\hat{m}_{r1},(\frac{1}{k_1\hat{\beta}_{r1}})(\frac{\beta_1-\beta_2}{\alpha_2-\alpha_1}))}{\Gamma(\hat{m}_{r1})} - \frac{(k_1\hat{\beta_{r1}})^{-\hat{m}_{r1}}}{\Gamma(\hat{m}_{r1})}\sum_{h=0}^{\infty}\frac{1}{\Gamma(\hat{m}_{s1}+h+1)}\left(\frac{1}{\hat{\beta}_{s1}}\right)^{\hat{m}_{s1}+h}e^{-\frac{\beta_1}{\hat{\beta}_{s1}}} \\ &\times\sum_{m=0}^{\infty}{}^{\hat{m}_{s1}+h}C_m\left(\frac{\beta_1}{\alpha_1}\right)^m\alpha_1^{\hat{m}_{s1}+h}\frac{\Gamma\left(\hat{m}_{s1}+\hat{m}_{r1}+h-m,(\frac{\alpha_1}{\hat{\beta}_{s1}}+\frac{1}{k_1\hat{\beta}_{r1}})(\frac{\beta_1-\beta_2}{\alpha_2-\alpha_1})\right)}{(\frac{\alpha_1}{\hat{\beta}_{s1}}+\frac{1}{k_1\hat{\beta}_{r1}})^{\hat{m}_{s1}+\hat{m}_{r1}+h-m}}\Bigg)\Bigg]\Bigg] \\ &\times\Bigg[\Bigg(1-\frac{(k_2\hat{\beta_{rr}})^{-\hat{m}_{rr}}}{\Gamma(\hat{m}_{rr})}\sum_{i=0}^{\infty}\frac{1}{\Gamma(\hat{m}_{sr}+i+1)}\left(\frac{1}{\rho_s\psi^{FD}\hat{\beta}_{sr}}\right)^{\hat{m}_{sr}+i}e^{-\frac{\delta_1}{\rho_s\psi^{FD}\hat{\beta}_{sr}}}(\rho_r)^{\hat{m}_{sr}+i}\sum_{n=0}^{\infty}{}^{\hat{m}_{sr}+i}C_n\left(\frac{\delta_1}{\rho_r}\right)^n \\ &\times\frac{\Gamma(\hat{m}_{sr}+\hat{m}_{rr}+i-n)}{(\frac{\rho_r}{\rho_s\psi^{FD}\hat{\beta}_{sr}}+\frac{1}{k_2\hat{\beta}_{rr}})^{\hat{m}_{sr}+\hat{m}_{rr}+i-n}}\Bigg)\times\Bigg(1-e^{-\frac{u_2^{FD}\delta_2}{\rho_r\hat{\beta_{r2}}}}\sum_{l=0}^{\infty}\frac{1}{\Gamma(\hat{m}_{r2}+l+1)}\left(\frac{u_2^{FD}\delta_2}{\rho_r\hat{\beta_{r2}}}\right)^{\hat{m}_{r2}+l}\Bigg)\Bigg]\Bigg] \end{aligned} \tag{31}$$

Proposition 5: With $k_1 \neq 0$, an approximate closed-form expression for $E[R_2^{FD}]$ obtained by using Gaussian-Chebyshev quadrature is given by

$$E[R_2^{FD}] \cong \frac{(k_2\beta_{rr})^{-m_{rr}}}{\Gamma(m_{rr})}\frac{(k_1\hat{\beta}_{r1})^{-\hat{m}_{r1}}}{\Gamma(\hat{m}_{r1})}\sum_{j=0}^{\hat{m}_{s1}-1}\frac{1}{j!}\sum_{i=0}^{j}{}^{j}C_i \times\left(\frac{\delta_4}{\rho_r}\right)^{j-i}(i+\hat{m}_{r1}-1)!\sum_{l=0}^{\hat{m}_{sr}-1}\frac{1}{l!}\left(\frac{1}{\rho_r}\right)^{l} \times\sum_{k=0}^{l}{}^{l}C_k\left(\frac{\delta_1}{\rho_r}\right)^{l-k}(m_{rr}+k-1)!\sum_{q=0}^{\hat{m}_{r2}-1}\frac{1}{q!}\frac{\pi}{Nln2} \times\sum_{n=1}^{N}\frac{d_n e_n f_n g_n q_n}{r_n}e^{-s_n}e^{-t_n}e^{-v_n} \tag{40}$$

where

$$d_n = \Big(\frac{a_2(\phi_n+1)\rho_r}{a_2(1-\phi_n)\rho_s\hat{\beta_{s1}}}\Big)^j\sqrt{1-\phi_n^2},$$
$$e_n = \Big(\frac{a_2(\phi_n+1)\rho_r}{a_2(1-\phi_n)\rho_s\hat{\beta}_{sr}}\Big)^l,$$
$$f_n = \left(\frac{\rho_r a_2(1+\phi_n)}{a_2(1-\phi_n)\rho_s\hat{\beta}_{sr}}+\frac{1}{k_2\beta_{rr}}\right)^{-m_{rr}-k},$$
$$g_n = \Big(\frac{\delta_2\, a_2(\phi_n+1)}{2\, a_1\rho_r\hat{\beta}_{r2}}\Big)^q,$$
$$q_n = \left(\frac{\rho_r a_2(1+\phi_n)}{a_2(1-\phi_n)\rho_s\hat{\beta}_{s1}}+\frac{1}{k_1\hat{\beta}_{r1}}\right)^{-\hat{m}_{r1}-j},$$
$$s_n = \Big(\frac{a_2(\phi_n+1)\rho_r}{a_2(1-\phi_n)\rho_s\hat{\beta}_{sr}}\Big),\quad t_n = \Big(\frac{a_2(\phi_n+1)\delta_3}{a_2(1-\phi_n)\rho_s\hat{\beta_{s1}}}\Big),$$
$$v_n = \frac{\delta_2\, a_2(\phi_n+1)}{2\, a_1\rho_r\hat{\beta}_{r2}},\quad r_n = \frac{2\, a_1+a_2(\phi_n+1)}{2\, a_1},$$
$$\phi_n = cos\Big(\frac{(2n-1)\pi}{2N}\Big)$$

and N is the complexity accuracy trade-off parameter.

Remark 4: With $k_1 = 0$, an approximate closed-form expression for $E[R_2^{FD}]$ obtained by using Gaussian-Chebyshev quadrature is given by

$$E[R_2^{FD}] \cong \frac{(k_2\beta_{rr})^{-m_{rr}}}{\Gamma(m_{rr})}\sum_{j=0}^{\hat{m}_{s1}-1}\frac{1}{j!}\sum_{l=0}^{\hat{m}_{sr}-1}\frac{1}{l!}\left(\frac{1}{\rho_r}\right)^{l}\sum_{k=0}^{l}{}^{l}C_k \times\left(\frac{\delta_1}{\rho_r}\right)^{l-k}(m_{rr}+k-1)!\sum_{q=0}^{\hat{m}_{r2}-1}\frac{1}{q!} \times\frac{\pi}{Nln2}\sum_{n=1}^{N}\frac{w_n e_n f_n g_n}{r_n}e^{-s_n}e^{-t_n}e^{-v_n} \tag{41}$$

where $w_n = \big(\frac{a_2(\phi_n+1)\delta_3}{a_2(1-\phi_n)\rho_s\hat{\beta_{s1}}}\big)^j\sqrt{1-\phi_n^2}$. Further, e_n, f_n, g_n, r_n, s_n, t_n, v_n, ϕ_n and N are defined as above.

Proof: Refer Appendix E.

Corollary 5: Following the procedure detailed in Appendix E, ergodic rate of U_2 in NOMA-HD-CDRT can be determined by utilizing the expressions for Γ_{12}^{HD}, Γ_{r2}^{HD} and Γ_{22}^{HD} given by (14), (12) and (13) respectively. Thus $E[R_2^{HD}]$ can be approximated as follows:

$$E[R_2^{HD}] \cong \sum_{l=0}^{\hat{m}_{sr}-1}\frac{1}{l!}\sum_{q=0}^{\hat{m}_{r2}-1}\frac{1}{q!}\frac{\pi}{N(2ln2)}\sum_{n=1}^{N}\frac{e_n g_n}{r_n}e^{-s_n}e^{-v_n} \tag{42}$$

V. SYSTEM OUTAGE PROBABILITY MINIMIZATION UNDER I-CSI

In this section, our aim is to find the optimal power allocation (OPA) factor $a_{1,opt}^{FD/HD}$ that minimizes the system outage probability in the considered network. For the analysis of OPA, we ignore the interference generated at U_1 by R's transmission to U_2 (i.e., we set $k_1 = 0$). Thus the minimization problem can be defined as follows:

$$\begin{aligned}&\min_{a_1} P_{out,sys}^{FD/HD}\\ &s.t.\ a_1+a_2=1\end{aligned} \tag{43}$$

where $P_{out,sys}^{FD}$ and $P_{out,sys}^{HD}$ are given by (30) and (33) respectively.

Proposition 6: The OPA coefficient $a_{1,opt}^{FD}$ that minimizes $P_{out,sys}^{FD}$ of NOMA-FD-CDRT network under I-CSI is given by

$$a_{1,opt}^{FD} = \frac{-B-\sqrt{B^2-4AC}}{2A} \tag{44}$$

where $A = -u_1^{FD}\sigma_{s1}^2\rho_s - u_1^{FD}\sigma_{s1}^2\rho_s u_2^{FD}$, $B = u_1^{FD}\sigma_{s1}^2\rho_s - u_1^{FD} - u_1^{FD}u_2^{FD} - u_2^{FD}\delta_3$ and $C = u_1^{FD}$.

Proof: From (30), $P_{out,sys}^{FD} \triangleq 1-(A_0\times B_0\times C_0)$ where A_0, B_0 and C_0 are given as:

$$A_0 = e^{-\frac{1}{\phi^{FD}\rho_s\hat{\beta}_{s1}}}\sum_{j=0}^{\hat{m}_{s1}-1}\frac{1}{j!}\left(\frac{1}{\phi^{FD}\rho_s\hat{\beta}_{s1}}\right)^j \tag{45a}$$

$$B_0 = e^{-\frac{\delta_1}{\rho_s\psi^{FD}\hat{\beta}_{sr}}}\frac{(k_2\beta_{rr})^{-m_{rr}}}{\Gamma(m_{rr})}\sum_{k=0}^{\hat{m}_{sr}-1}\left(\frac{\rho_r}{\rho_s\psi^{FD}\hat{\beta}_{sr}}\right)^k \times\sum_{l=0}^{k}{}^{k}C_l\left(\frac{\delta_1}{\rho_r}\right)^{k-l}(l+m_{rr}-1)! \times\left(\frac{\rho_r}{\rho_s\psi^{FD}\hat{\beta}_{sr}}+\frac{1}{k_2\beta_{rr}}\right)^{-l-m_{rr}} \tag{45b}$$

$$C_0 = e^{-\frac{u_2^{FD}\delta_2}{\rho_r\hat{\beta_{r2}}}}\sum_{i=0}^{\hat{m}_{r2}-1}\frac{1}{i!}\left(\frac{u_2^{FD}\delta_2}{\rho_r\hat{\beta_{r2}}}\right)^i \tag{45c}$$

In (45b), $\psi^{FD} = \frac{a_2-u_2^{FD}a_1}{u_2^{FD}} > 0$ which implies $a_2 > a_1u_2^{FD}$. Since $a_2 = 1-a_1$, this implies $a_1 < \frac{1}{1+u_2^{FD}}$.

Now consider A_0, where $\phi^{FD} = \min\left\{\frac{a_2-u_2^{FD}a_1}{u_2^{FD}\delta_3}, \frac{a_1-\beta a_2\, u_1^{FD}}{u_1^{FD}\delta_4}\right\}$. Let us assume $\beta = 0$ (i.e., P-SIC) which implies $\phi^{FD} = min\left\{\frac{a_2-u_2^{FD}a_1}{u_2^{FD}\delta_3}, \frac{a_1}{u_1^{FD}\delta_4}\right\}$. This gives rise to two distinct cases as given below:

Case(i): $\frac{a_2-u_2^{FD}a_1}{u_2^{FD}\delta_3} < \frac{a_1}{u_1^{FD}\delta_4}$ while $a_1 < \frac{1}{1+u_2^{FD}}$. Since $a_2 = 1-a_1$, this implies that $a_1 < \frac{1}{1+u_2^{FD}+\frac{u_2^{FD}\delta_3}{u_1^{FD}\delta_4}}$ where $\delta_3 = \sigma_{s1}^2\rho_s + 1$ and $\delta_4 = \sigma_{s1}^2\rho_s a_1 + 1$. Substituting for δ_4, the following condition can be imposed on a_1, i.e., $\frac{-B-\sqrt{B^2-4AC}}{2A} < a_1 < \frac{1}{1+u_2^{FD}}$, where $A = -u_1^{FD}\sigma_{s1}^2\rho_s - u_1^{FD}\sigma_{s1}^2\rho_s u_2^{FD}$, $B = u_1^{FD}\sigma_{s1}^2\rho_s - u_1^{FD} - u_1^{FD}u_2^{FD} - u_2^{FD}\delta_3$ and $C = u_1^{FD}$. Thus we write $P_{out,sys}^{FD}$ as $P_{out,sys}^{FD}(a_1) = 1-[A_0(a_1)\times B_0(a_1)\times C_0]$ where $A_0(a_1)$ and $B_0(a_1)$ are given by

$$A_0(a_1) = e^{-\frac{u_2^{FD}\delta_3}{(1-a_1-u_2^{FD}a_1)\rho_s\hat{\beta}_{s1}}}\sum_{j=0}^{\hat{m}_{s1}-1}\frac{1}{j!}\times\left(\frac{u_2^{FD}\delta_3}{(1-a_1-u_2^{FD}a_1)\rho_s\hat{\beta}_{s1}}\right)^j \tag{46a}$$

$$\begin{aligned}B_0(a_1) &= e^{-\frac{\delta_1 u_2^{FD}}{\rho_s(1-a_1-a_1u_2^{FD})\hat{\beta}_{sr}}}\frac{(k_2\beta_{rr})^{-m_{rr}}}{\Gamma(m_{rr})}\\ &\times\sum_{j=0}^{\hat{m}_{sr}-1}\left(\frac{\rho_r u_2^{FD}}{\rho_s(1-a_1-a_1u_2^{FD})\hat{\beta}_{sr}}\right)^j\sum_{l=0}^{j}{}^jC_l\left(\frac{\delta_1}{\rho_r}\right)^{j-l}\\ &\times(l+m_{rr}-1)!\left(\frac{\rho_r u_2^{FD}}{\rho_s(1-a_1-a_1u_2^{FD})\hat{\beta}_{sr}}+\frac{1}{k_2\beta_{rr}}\right)^{-l-m_{rr}}\end{aligned} \tag{46b}$$

Notice that $A_0(a_1)$ and $B_0(a_1)$ are obtained as above by substituting $\phi^{FD} = \frac{1-a_1-u_2^{FD}a_1}{u_2^{FD}\delta_3}$ and $\psi^{FD} = \frac{1-a_1-a_1u_2^{FD}}{u_2^{FD}}$ in (45a) and (45b) respectively. The first order derivative of $[P_{out,sys}^{FD}(a_1)]$ with respect to a_1 is given by

$$[P_{out,sys}^{FD}(a_1)]' = -C_0([A_0(a_1)]'B_0(a_1) + A_0(a_1)[B_0(a_1)]') \tag{47}$$

where $[A_0(a_1)]'$ and $[B_0(a_1)]'$ are the first derivative of $A_0(a_1)$ and $B_0(a_1)$ respectively. Now $[A_0(a_1)]' = x(a_1)+y(a_1)$ where $x(a_1)$ and $y(a_1)$ are given by

$$\begin{aligned}x(a_1) &= -\frac{\frac{u_2^{FD}\delta_3}{\rho_s\hat{\beta}_{s1}}(1+u_2^{FD})e^{\frac{u_2^{FD}\delta_3}{\rho_s\hat{\beta}_{s1}}(u_2^{FD}a_1+a_1-1)}}{(-u_2^{FD}a_1-a_1+1)^2}\\ &\quad\times\sum_{j=0}^{\hat{m}_{s1}-1}\frac{1}{j!}\left(\frac{u_2^{FD}\delta_3}{(1-a_1-u_2^{FD}a_1)\rho_s\hat{\beta}_{s1}}\right)^j\end{aligned} \tag{48a}$$

$$\begin{aligned}y(a_1) &= e^{-\frac{u_2^{FD}\delta_3}{(1-a_1-u_2^{FD}a_1)\rho_s\hat{\beta}_{s1}}}\sum_{j=0}^{\hat{m}_{s1}-1}\frac{1}{j!}\\ &\quad\times\frac{\frac{-u_2^{FD}\delta_3}{\rho_s\hat{\beta}_{s1}}(-u_2^{FD}-1)j\left(\frac{u_2^{FD}\delta_3}{\rho_s\hat{\beta}_{s1}(-u_2^{FD}a_1-a_1+1)}\right)^{j-1}}{(-u_2^{FD}a_1-a_1+1)^2}\end{aligned} \tag{48b}$$

Similarly, $[B_0(a_1)]' = f(a_1)+g(a_1)+h(a_1)$ where $f(a_1)$, $g(a_1)$ and $h(a_1)$ are given by equations (49a), (49b) and (49c)

With the help of numerical investigations, it is observed that $[P_{out,sys}^{FD}(a_1)]' > 0$ for the range of a_1 considered. Thus we conclude that $P_{out,sys}^{FD}$ is a monotonically increasing function of a_1 in the interval $\frac{-B-\sqrt{B^2-4AC}}{2A} < a_1 < \frac{1}{1+u_2^{FD}}$.

Case(ii): $\frac{a_1}{u_1^{FD}\delta_4} < \frac{a_2-u_2^{FD}a_1}{u_2^{FD}\delta_3}$. Since $a_2 = 1-a_1$ and $\delta_4 = \sigma_{s1}^2\rho_s a_1+1$, the above implies $0 < a_1 < \frac{-B-\sqrt{B^2-4AC}}{2A}$. In this case, let $P_{out,sys}^{FD} = 1-[A_1(a_1)\times B_0(a_1)\times C_0]$ where $B_0(a_1)$ is given by (46b) while $A_1(a_1)$ is obtained by substituting $\phi^{FD} = \frac{a_1}{u_1^{FD}(\sigma_{s1}^2\rho_s a_1+1)}$ in the expression for A_0 given by (45a), as:

$$A_1(a_1) = e^{-\frac{u_1^{FD}(\sigma_{s1}^2\rho_s a_1+1)}{\rho_s\hat{\beta}_{s1}a_1}}\sum_{j=0}^{\hat{m}_{s1}-1}\frac{1}{j!}\left(\frac{u_1^{FD}(\sigma_{s1}^2\rho_s a_1+1)}{\rho_s\hat{\beta}_{s1}a_1}\right)^j \tag{50}$$

The first order derivative of $P_{out,sys}^{FD}$ can be computed as $[P_{out,sys}^{FD}(a_1)]' = -C_0([A_1(a_1)]'B_0(a_1) + A_1(a_1)[B_0(a_1)]')$ where $[B_0(a_1)]'$ has been determined under case (i) above, which is obtained by combining (49a)-(49c), as shown at the bottom of the next page. Now $[A_1(a_1)]'$ can be written as $A_1[(a_1)]' = u(a_1)+v(a_1)$ where $u(a_1)$ and $v(a_1)$ are given by

$$u(a_1) = \frac{u_1^{FD}e^{-\frac{u_1^{FD}(\sigma_{s1}^2\rho_s a_1+1)}{\rho_s\hat{\beta}_{s1}a_1}}}{\rho_s\hat{\beta}_{s1}a_1^2}\sum_{j=0}^{\hat{m}_{s1}-1}\frac{1}{j!}\times\left(\frac{u_1^{FD}(\sigma_{s1}^2\rho_s a_1+1)}{\rho_s\hat{\beta}_{s1}a_1}\right)^j \tag{51a}$$

$$v(a_1) = e^{-\frac{u_1^{FD}(\sigma_{s1}^2\rho_s a_1+1)}{\rho_s\hat{\beta}_{s1}a_1}}\sum_{j=0}^{\hat{m}_{s1}-1}\frac{1}{j!}\times\frac{-u_1^{FD}j\left(\frac{u_1^{FD}(\sigma_{s1}^2\rho_s a_1+1)}{\rho_s\hat{\beta}_{s1}a_1}\right)^{j-1}}{\rho_s\hat{\beta}_{s1}a_1^2} \tag{51b}$$

Through numerical investigations, we observe that $[P_{out,sys}^{FD}(a_1)]' < 0$ for the range of a_1 considered. Thus $P_{out,sys}^{FD}$ is a decreasing function of a_1 for $0 < a_1 < \frac{-B-\sqrt{B^2-4AC}}{2A}$. Accordingly, $P_{out,sys}^{FD}$ is a monotonically decreasing function of a_1 for $0 < a_1 < \frac{-B-\sqrt{B^2-4AC}}{2A}$ and monotonically increasing function of a_1 for $\frac{-B-\sqrt{B^2-4AC}}{2A} < a_1 < \frac{1}{1+u_2^{FD}}$. Hence the OPA coefficient $a_{1,opt}^{FD}$ that minimizes the system outage is obtained as $a_{1,opt}^{FD} = \frac{-B-\sqrt{B^2-4AC}}{2A}$. Proposition 6 is thus proved.

Corollary 6: As a continuation of proposition 6, the OPA coefficient $a_{1,opt}^{HD}$ that minimizes the system outage of NOMA-HD-CDRT network under the influence of I-CSI can also be determined. For this, we write $P_{out,sys}^{HD}$ given by (33) as $P_{out,sys}^{HD} = 1-(P_0\times Q_0\times R_0)$, where $P_0 = e^{-\frac{1}{\phi^{HD}\rho_s\hat{\beta}_{s1}}}\sum_{j=0}^{\hat{m}_{s1}-1}\frac{1}{j!}\left(\frac{1}{\phi^{HD}\rho_s\hat{\beta}_{s1}}\right)^j$, $Q_0 = e^{-\frac{\delta_1}{\rho_s\psi^{HD}\hat{\beta}_{sr}}}\sum_{k=0}^{\hat{m}_{sr}-1}\frac{1}{k!}\left(\frac{\delta_1}{\rho_s\psi^{HD}\hat{\beta}_{sr}}\right)^k$ and $R_0 = e^{-\frac{u_2^{HD}\delta_2}{\rho_r\hat{\beta}_{r2}}}\times\sum_{i=0}^{\hat{m}_{r2}-1}\frac{1}{i!}\left(\frac{u_2^{HD}\delta_2}{\rho_r\hat{\beta}_{r2}}\right)^i$. Adopting the procedure outlined above,

$a_{1,opt}^{HD}$ can be obtained as:

$$a_{1,opt}^{HD} = \frac{-E - \sqrt{E^2 - 4DF}}{2D} \tag{52}$$

where $D = -u_1^{HD}\sigma_{s1}^2\rho_s - u_1^{HD}\sigma_{s1}^2\rho_s u_2^{HD}$, $E = u_1^{HD}\sigma_{s1}^2\rho_s - u_1^{HD} - u_1^{HD}u_2^{HD} - u_2^{HD}\delta_3$ and $F = u_1^{HD}$.

VI. NUMERICAL AND SIMULATION RESULTS

Here we describe the results of our investigations. The analytical results are validated by Monte-Carlo simulations considering a set of 10^5 channel realizations. We consider a 2-D topology for the network with $(x_i; y_i)$ representing the coordinates of node i. Unless specified otherwise, we assume BS, R, U_2 and U_1 to be placed at (0,0); (0.25,0); (0.5,0); and (0.25,1) respectively, so that the distances between the nodes are: $d_{s1} = 1.03d_0$, $d_{sr} = 0.5d_0$, $d_{r2} = 0.5d_0$, where d_0 (i.e., reference distance) = 1 km. Further, we set $r_1 = 0.3$ bpcu, $r_2 = 0.3$ bpcu, $a_1 = 0.3$, $\hat{m}_{ij} = 2$, $\sigma_{s1}^2 = \sigma_{sr}^2 = \sigma_{r2}^2 = \sigma_e^2 = 0.001$, $\beta = 0.3$, $n = 3$ and we set $\rho_r = \rho_s = \rho$. In the figures 'Sim' represents the result of Monte-Carlo simulations, while 'Ana' represents the results obtained from the analytical model.

A. EVALUATION OF OUTAGE PROBABILITIES OF U_1 AND U_2

FIGURE 2 compares the outage experienced by U_1 and U_2 (in NOMA-FD-CDRT network) under I-CSI/I-SIC and P-CSI/P-SIC. Notice that, here we assume residual interference from R to U_1 to be zero (i.e., $k_1 = 0$). Results show that P_{out} of U_1 and U_2 become significantly higher under I-CSI/I-SIC. When transmit power (ρ) becomes higher, U_2 suffers outage floor under both P-CSI/P-SIC as well as I-CSI/I-SIC. For larger ρ, the mean RSI power (π_{rr}) increases, which leads to outage floor for U_2. Successful decoding of x_1 at U_1 is not affected by RSI; thus under P-CSI/P-SIC, U_1 does not experience outage floor in the high ρ region. However, U_1 suffers outage floor under I-CSI/I-SIC, since larger ρ increases the residual interference generated by I-SIC at U_1. For the entire range of ρ considered in FIGURE 2, $P_{out,1}^{FD} > P_{out,2}^{FD}$, since the power allocation coefficient at BS (a_1) has been chosen arbitrarily, i.e., symbol x_2 has been allocated higher power at BS. The P_{out} of U_1 and U_2 under OMA are also shown in FIGURE 2. Under OMA, BS transmits x_1 to U_1 in time slot #1, which is decoded in the same time slot. In time slot #2, BS transmits x_2 and the DF relay (R) simultaneously forwards x_2 to U_2. Since OMA requires two time slots, the achievable rate gets halved. For outage comparison, both OMA and NOMA have to achieve the same target rates; thus the threshold SINR is higher for OMA, which makes the P_{out} of U_1 and U_2 to be higher under OMA, as compared to NOMA.

FIGURE 3 compares the P_{out} of U_1 and U_2 in FD/HD systems under P-CSI/P-SIC and I-CSI/I-SIC. The outage probabilities of U_1 and U_2 are observed to be higher in NOMA-HD-CDRT system, in the low transmit power region, as compared to that observed in NOMA-FD-CDRT system.

$$f(a_1) = -\frac{\frac{u_2^{FD}\delta_1}{\rho_s\hat{\beta}_{sr}}(1+u_2^{FD})e^{\frac{u_2^{FD}\delta_1}{\rho_s\hat{\beta}_{sr}}(u_2^{FD}a_1+a_1-1)}}{(-u_2^{FD}a_1 - a_1 + 1)^2}\frac{(k_2\beta_{rr})^{-m_{rr}}}{\Gamma(m_{rr})}$$
$$\times\sum_{j=0}^{\hat{m}_{sr}-1}\left(\frac{\rho_r u_2^{FD}}{\rho_s(1-a_1-a_1u_2^{FD})\hat{\beta}_{sr}}\right)^j\sum_{l=0}^{j}{}^jC_l\left(\frac{\delta_1}{\rho_r}\right)^{j-l}\times(l+m_{rr}-1)!\left(\frac{\rho_r u_2^{FD}}{\rho_s(1-a_1-a_1u_2^{FD})\hat{\beta}_{sr}}+\frac{1}{k_2\beta_{rr}}\right)^{-l-m_{rr}} \tag{49a}$$

$$g(a_1) = e^{-\frac{\delta_1 u_2^{FD}}{\rho_s(1-a_1-a_1u_2^{FD})\hat{\beta}_{sr}}}\frac{(k_2\beta_{rr})^{-m_{rr}}}{\Gamma(m_{rr})}$$
$$\times\sum_{j=0}^{\hat{m}_{sr}-1}\frac{\frac{-u_2^{FD}\rho_r}{\rho_s\hat{\beta}_{sr}}(-u_2^{FD}-1)j\left(\frac{u_2^{FD}\rho_r}{\rho_s\hat{\beta}_{sr}(-u_2^{FD}a_1-a_1+a)}\right)^{j-1}}{(-u_2^{FD}a_1-a_1+1)^2}\times\sum_{l=0}^{j}{}^jC_l\left(\frac{\delta_1}{\rho_r}\right)^{j-l}(l+m_{rr}-1)!$$
$$\left(\frac{\rho_r u_2^{FD}}{\rho_s(1-a_1-a_1u_2^{FD})\hat{\beta}_{sr}}+\frac{1}{k_2\beta_{rr}}\right)^{-l-m_{rr}} \tag{49b}$$

$$h(a_1) = e^{-\frac{\delta_1 u_2^{FD}}{\rho_s(1-a_1-a_1u_2^{FD})\hat{\beta}_{sr}}}\frac{(k_2\beta_{rr})^{-m_{rr}}}{\Gamma(m_{rr})}$$
$$\times\sum_{j=0}^{\hat{m}_{sr}-1}\left(\frac{\rho_r u_2^{FD}}{\rho_s(1-a_1-a_1u_2^{FD})\hat{\beta}_{sr}}\right)^j\sum_{l=0}^{j}{}^jC_l\left(\frac{\delta_1}{\rho_r}\right)^{j-l}$$
$$\times(l+m_{rr}-1)!\times\frac{\frac{\rho_r u_2^{FD}}{\rho_s\hat{\beta}_{sr}}(-u_2^{FD}-1)(l+m_{rr})\left(\frac{\rho_r u_2^{FD}}{\rho_s\hat{\beta}_{sr}(-u_2^{FD}a_1-a_1+1)}+\frac{1}{k_2\beta_{rr}}\right)^{-l-m_{rr}-1}}{-u_2^{FD}a_1-a_1+1} \tag{49c}$$

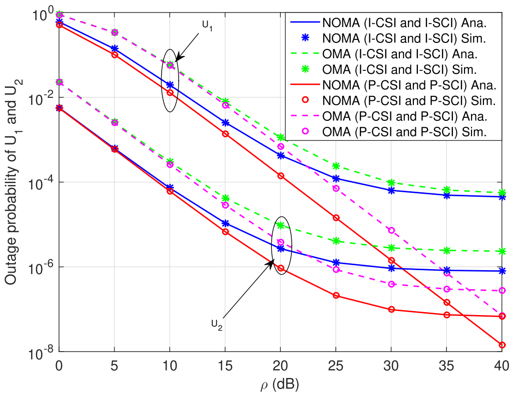

FIGURE 2. Outage probability of U_1 and U_2 in NOMA-FD-CDRT network v/s ρ ($\beta = 0.3, \sigma_e^2 = 0.009, r_1 = 0.3, r_2 = 0.3$, $RSI = -3$ dB, $k_1 = 0$, $a_1 = 0.3$).

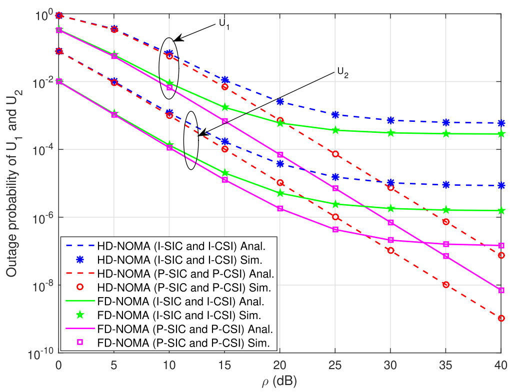

FIGURE 3. Outage probability of U_1 and U_2 in NOMA-FD/HD-CDRT network v/s ρ ($\beta = 0.3, \sigma_e^2 = 0.009, r_1 = 0.3, r_2 = 0.3$, $RSI = -3$ dB, $k_1 = 10^{-2}$, $a_1 = 0.4648$).

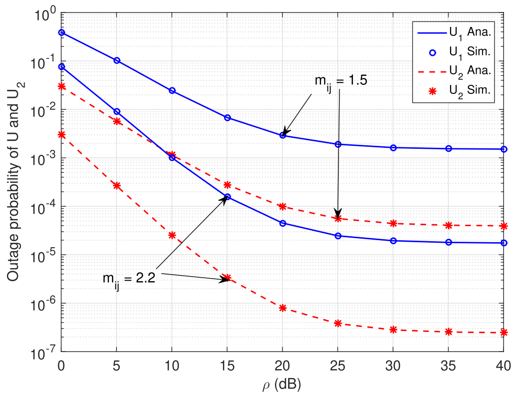

FIGURE 4. Outage probability of U_1 and U_2 in NOMA-FD/HD-CDRT network v/s ρ: for non-integer values of $\hat{m}_{ij}$ ($\beta = 0.3, \sigma_e^2 = 0.009$, $r_1 = 0.3, r_2 = 0.3$, $RSI = -3$ dB, $k_1 = 10^{-2}$, $a_1 = 0.4648$).

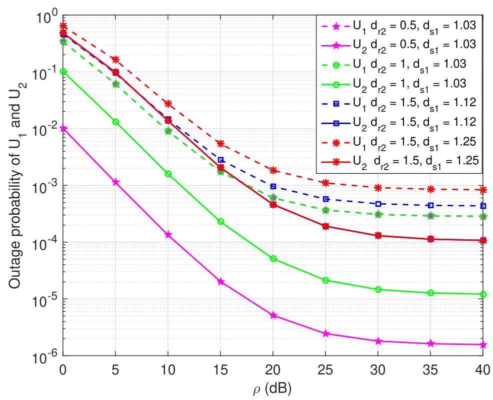

FIGURE 5. Outage probability of U_1 and U_2 in NOMA-FD/HD-CDRT network v/s ρ: Distinct distances ($\beta = 0.3, \sigma_e^2 = 0.009, r_1 = 0.3, r_2 = 0.3$, $RSI = -3$ dB, $k_1 = 10^{-2}$, $a_1 = 0.4648$).

When R operates in HD mode, two time slots are needed to complete the transmission of x_1 and x_2 in the system. For outage comparison, both HD and FD systems have to achieve the same target rates; thus the threshold SINR requirement is higher for HD systems, which makes P_{out} of U_1 and U_2 to be higher in NOMA-HD-CDRT system. For very large ρ, both U_1 and U_2 suffers an outage floor in NOMA-FD-CDRT network under both P-CSI/P-SIC as well as I-CSI/I-SIC. Here U_2 suffers outage floor, owing to the higher level of interference created by RSI and I-SIC. The near user U_1 suffers outage floor under P-CSI/P-SIC due to the interference generated at U_1 by R's transmission to U_2, which becomes very high when ρ is increased. It suffers outage floor under I-CSI/I-SIC as well due to the combined effect of residual interference and I-SIC. In NOMA-HD-CDRT network, U_1 and U_2 suffer from outage floor under I-CSI/I-SIC alone, i.e., outage floor is absent under P-CSI/P-SIC since HD networks do not suffer from RSI, and other interference effects.

Now, FIGURE 4 shows the outage probabilities user 1 and user 2, with non-integer values for $\hat{m}_{ij}$. Here we assume $\hat{m}_{ij} \forall i, j$ to be equal. The results show that the outage improves significantly, when $\hat{m}_{ij}$ is increased. FIGURE 5 shows the outage results which are obtained by changing the locations of U_2 and U_1, i.e., for distinct values of d_{r2} and d_{s1}. As d_{r2} is increased, $P_{out,2}$ becomes higher, while increase of d_{s1} makes $P_{out,1}$ to become higher. The results thus show that the analytical model can be applied to find the outage and other metrics when the position of the nodes are changed. FIGURE 6 and FIGURE 7 respectively show the impact of channel estimation error variance (σ_e^2) and I-SIC factor (β) on the P_{out} of U_1 and U_2 in NOMA-FD-CDRT network. As σ_e^2 increases from 0.001 to 0.005, $P^{FD}_{out,1}$ increases by 82%, while $P^{FD}_{out,2}$ increases by 67%. As β increases, residual interference due to I-SIC increases $P^{FD}_{out,1}$; however β does not influence $P^{FD}_{out,2}$ since U_2 does not suffer from interference due to I-SIC. For $\rho = 20$ dB, increase of β from 0.2 to 0.4 makes $P^{FD}_{out,1}$ to increase by 97%. Results in FIGURE 7 further show that higher mean RSI power (π_{rr}) increases $P^{FD}_{out,2}$ significantly owing to the SINR degradation over the BS-R link. With $\rho = 30$ dB, increase of π_{rr} from -15 dB to -3 dB makes $P^{FD}_{out,2}$ to increase by 90%.

FIGURE 8 and FIGURE 9 show P_{out} of U_1 and U_2 (in NOMA-FD-CDRT network) against a_1 for various values of σ_e^2, β, r_1, r_2 and π_{rr}. As a_1 increases, $P^{FD}_{out,1}$ decreases, while $P^{FD}_{out,2}$ becomes higher owing to the larger power allocation at the BS for the symbol x_1. However, $P^{FD}_{out,1}$ tends to unity when $u_2^{FD} > a_2/a_1$ or when $u_1^{FD} > a_1/\beta a_2$ while $P^{FD}_{out,2}$ becomes

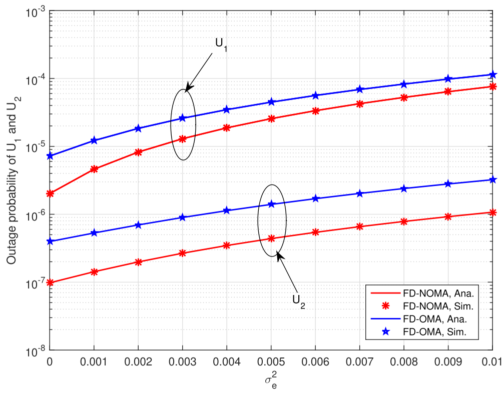

FIGURE 6. Outage probability of U_1 and U_2 under I-CSI/I-SIC in NOMA-FD-CDRT system v/s σ_e^2 (ρ = 30dB, β = 0.3, r_1 = 0.5, r_2 = 0.5, k_1 = 0).

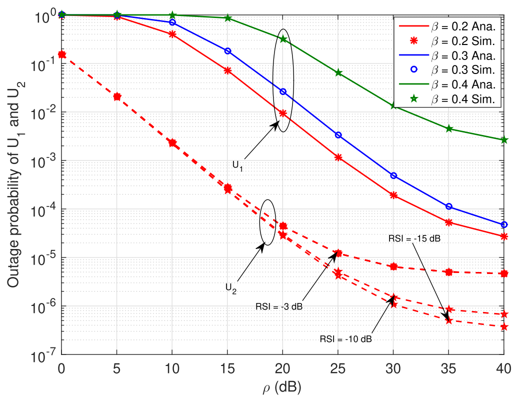

FIGURE 7. Outage probability in NOMA-FD-CDRT system v/s ρ for distinct β (r_1 = 1, r_2 = 1, σ_e^2 = 0.001, k_1 = 0).

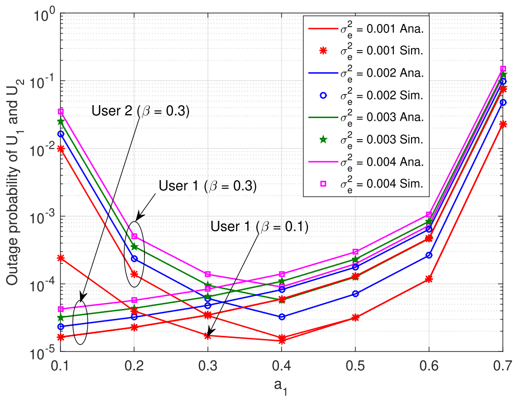

FIGURE 8. Outage probability in NOMA-FD-CDRT system v/s a_1 (ρ = 30 dB, RSI = -3 dB, r_1 = 0.5, r_2 = 0.5, k_1 = 0).

unity when $u_2^{FD} > a_2/a_1$. For certain values of a_1 (i.e., $a_{1,fair}^{FD}$), P_{out} of U_1 and U_2 can be made equal, (i.e., $P_{out,1}^{FD} = P_{out,2}^{FD}$) and these values are listed in Tables 1(a) and 1(b). When the I-SIC factor β increases, $P_{out,1}^{FD}$ becomes higher; to satisfy the equal outage criterion, $a_{1,fair}^{FD}$ shall be increased. Further, increase of π_{rr} makes $P_{out,2}^{FD}$ to be higher; thus to satisfy the equal outage criterion, $a_{2,fair}^{FD}$ shall be increased. Increase of target rate r_1 (keeping r_2 constant) makes $P_{out,1}^{FD}$ to be higher. To ensure the equal outage criterion, $a_{1,fair}^{FD}$

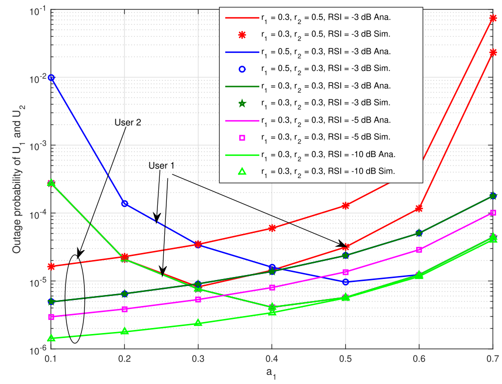

FIGURE 9. Outage probability in NOMA-FD-CDRT system v/s a_1 (ρ = 30 dB, σ_e^2 = 0.001, β = 0.3, k_1 = 0).

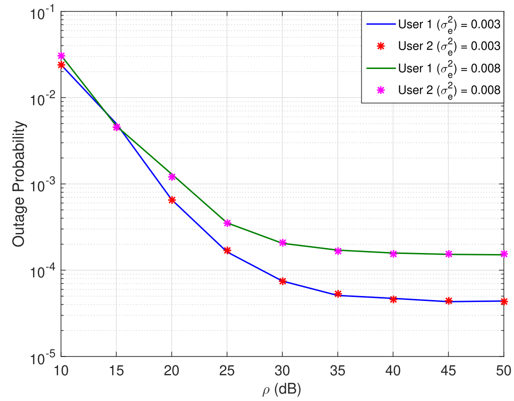

FIGURE 10. Outage probability with $a_1 = a_{1,fair}^{FD}$ v/s ρ (β = 0.3).

shall be increased. FIGURE 10 shows P_{out} of U_1 and U_2 by choosing $a_1 = a_{1,fair}^{FD}$ according to Table 1. Selection of $a_1 = a_{1,fair}^{FD}$ ensures $P_{out,1}^{FD} = P_{out,2}^{FD}$, over the entire range of ρ considered; thus fairness in terms of P_{out} can be ensured under I-CSI/I-SIC.

B. EVALUATION OF ERGODIC RATES

FIGURE 11 and FIGURE 12 respectively show the ergodic rates and the ergodic sum rate in NOMA-FD/HD-CDRT network. In FIGURE 11, ergodic rates $E[R_1^{FD}]$ and $E[R_2^{FD}]$ are plotted for distinct values of σ_e^2 and β. As σ_e^2 increases, both $E[R_1^{FD}]$ and $E[R_2^{FD}]$ decreases. When β is increased, $E[R_1^{FD}]$ decreases owing to the interference generated by I-SIC, while $E[R_2^{FD}]$ does not depend β. The ergodic rate achieved by the users in the FD system is higher than the equivalent HD system, where additional time slots are needed to complete the transmission of symbols. The ergodic sum rate results shown in FIGURE 12 are observed to be sensitive to the changes in σ_e^2 and β. When ρ becomes higher, NOMA-FD/HD-CDRT systems will become interference limited due to higher interference generated by RSI and I-SIC in FD systems and due to I-SIC in HD systems, which leads to saturation behavior for the ergodic rate plots. Moreover, it can be seen that non-zero values for k_1 introduce residual interference at U_1 (due to transmission from R). This effectively reduces the ergodic rates of the users and the ergodic sum rate as well.

TABLE 1. (a) $a^{FD}_{1,fair}$ that ensures $P^{FD}_{out,1} = P^{FD}_{out,2}$ (ρ = 30dB, RSI = −3 dB, $r_1 = r_2 = 0.5$). (b) $a^{FD}_{1,fair}$ that ensures $P^{FD}_{out,1} = P^{FD}_{out,2}$ (ρ = 30dB, $\beta = 0.3$, $\sigma_e^2 = 0.001$).

(a)

	$\sigma_e^2 = 0.001$				$\sigma_e^2 = 0.002$				$\sigma_e^2 = 0.003$				$\sigma_e^2 = 0.004$			
β	0.1	0.2	0.3	0.4	0.1	0.2	0.3	0.4	0.1	0.2	0.3	0.4	0.1	0.2	0.3	0.4
$a^{FD}_{1,fair}$	0.24	0.27	0.3	0.32	0.25	0.286	0.32	0.345	0.255	0.3	0.33	0.36	0.26	0.305	0.34	0.37

(b)

	$a^{FD}_{1,fair}$		
	$r_1 = 0.3, r_2 = 0.5$	$r_1 = 0.5, r_2 = 0.3$	$r_1 = 0.3, r_2 = 0.3$
$RSI = -3dB$	0.195	0.415	0.285
$RSI = -5dB$	0.23	0.465	0.33
$RSI = -10dB$	0.29	0.55	0.42

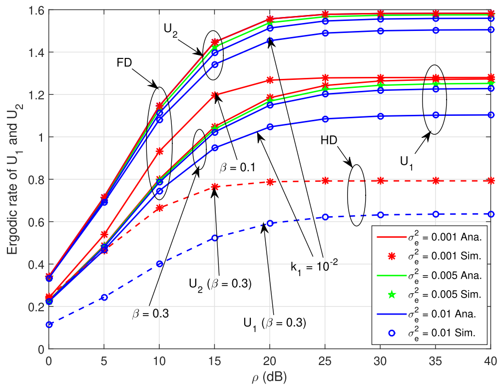

FIGURE 11. Ergodic rate of U_1 and U_2 v/s ρ in NOMA-FD/HD-CDRT network.

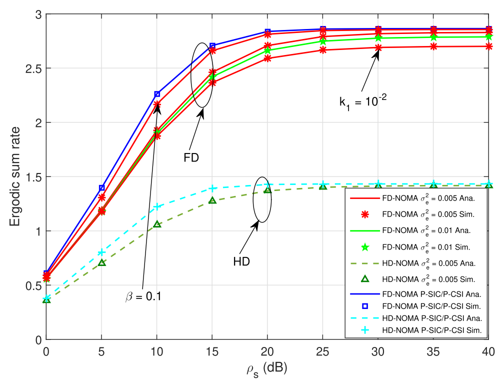

FIGURE 12. Ergodic sum rate of NOMA-FD/HD-CDRT network v/s ρ.

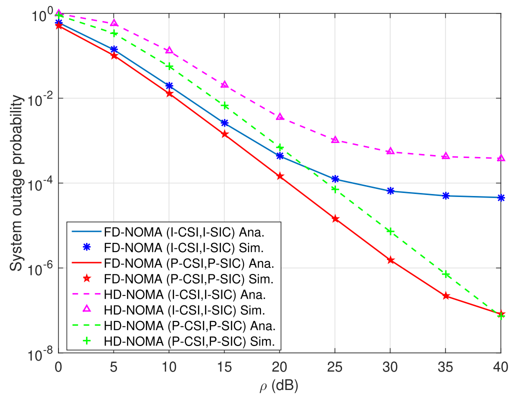

FIGURE 13. System outage probability of NOMA-FD/HD-CDRT network v/s ρ ($\beta = 0.3$, $\sigma_e^2 = 0.009$, $r_1 = 0.3$, $r_2 = 0.3$).

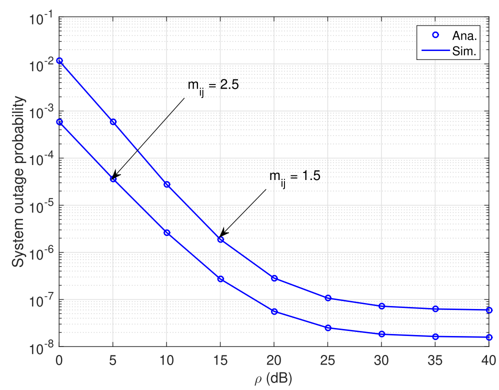

FIGURE 14. System outage probability in NOMA-FD/HD-CDRT network v/s ρ: non-integer values of $\hat{m}_{ij}$ ($\beta = 0.3$, $\sigma_e^2 = 0.009$, $r_1 = 0.3$, $r_2 = 0.3$, $RSI = -3$ dB, $k_1 = 10^{-2}$, $a_1 = 0.4648$).

C. EVALUATION OF SYSTEM OUTAGE PROBABILITY

The system outage probability ($P_{out,sys}$) results are shown in FIGURE 13 for NOMA-FD/HD-CDRT networks. When ρ is increased, $P_{out,sys}$ reduces; further, I-CSI/I-SIC leads to significant increase of $P_{out,sys}$, as compared to P-CSI/P-SIC. As seen earlier, HD network suffers from higher $P_{out,sys}$ as compared to FD network, owing to the requirement of higher threshold SINR for the latter. For very large ρ, NOMA-FD-CDRT network suffers from outage floor under both P-CSI/P-SIC and I-CSI/I-SIC, due to the combined effects of RSI and I-SIC. However, NOMA-HD-CDRT network suffers from outage floor under I-CSI/I-SIC alone, due to the interference generated by I-SIC, while outage floor is not observed under P-CSI/P-SIC (since RSI is absent in HD case). Now, FIGURE 14 shows system outage probability, with non-integer values for $\hat{m}_{ij}$. FIGURE 15 shows $P^{FD}_{out,sys}$ versus a_1, for distinct target rates r_1 and r_2. Notice that $P^{FD}_{out,sys}$ becomes higher either when a_1 is low or when a_1 becomes higher. When a_1 is low, U_1 will experience higher P_{out} whereas for higher values of a_1, U_2 suffers higher P_{out}; both these events lead to higher $P^{FD}_{out,sys}$. Further, an optimal a_1 ($a^{FD}_{1,opt}$) exists that minimizes $P^{FD}_{out,sys}$. Table 2 lists $a^{FD/HD}_{1,opt}$ that minimizes $P^{FD/HD}_{out,sys}$ and the corresponding $P^{opt,FD/HD}_{out,sys}$. When r_1 is higher (with r_2 fixed), $a^{FD/HD}_{1,opt}$ shall be increased to minimize $P^{opt,FD/HD}_{out,sys}$. Likewise, when r_2 is higher, (with

TABLE 2. Optimal a_1 that minimizes $P_{out,sys}$ in NOMA-FD/HD-CDRT network ($\rho = 30$ *dB*, *RSI* $= -3$ *dB*).

	$\sigma_e^2 = 0.001$				$\sigma_e^2 = 0.005$				$\sigma_e^2 = 0$			
Target rate	$a_{1,opt}^{HD}$	$a_{1,opt}^{FD}$	$P_{out,sys}^{opt,HD}$	$P_{out,sys}^{opt,FD}$	$a_{1,opt}^{HD}$	$a_{1,opt}^{FD}$	$P_{out,sys}^{opt,HD}$	$P_{out,sys}^{opt,FD}$	$a_{1,opt}^{HD}$	$a_{1,opt}^{FD}$	$P_{out,sys}^{opt,HD}$	$P_{out,sys}^{opt,FD}$
$r_1 = 1$, $r_2 = 0.5$	0.4041	0.5094	0.00025983	0.000023153	0.3702	0.4618	0.0135	0.00012687	0.4286	0.5469	0.00011748	0.000013050
$r_1 = 0.5$, $r_2 = 1$	0.1061	0.1625	0.0022	0.000023259	0.0552	0.0813	0.0105	0.00012782	0.1429	0.2265	0.00011773	0.000010378
$r_1 = 0.5$, $r_2 = 0.5$	0.2808	0.3446	0.000050255	0.0000069906	0.2000	0.2423	0.00024218	0.000035632	0.3333	0.4142	0.000021716	0.0000031033
$r_1 = 1$, $r_2 = 1$	0.1754	0.2808	0.00095342	0.000054838	0.1312	0.2000	0.0033	0.00024685	0.2000	0.3333	0.00053301	0.000027836

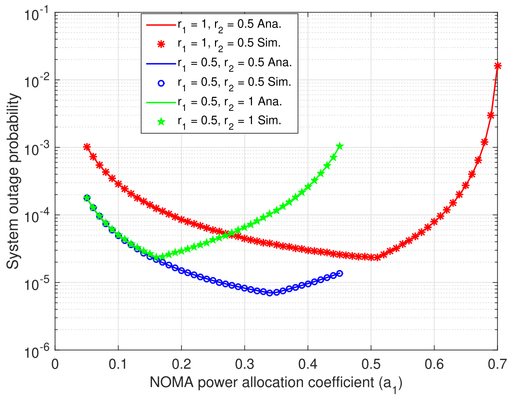

FIGURE 15. System outage probability of NOMA-FD-CDRT network v/s a_1 ($\sigma_e^2 = 0.001$, $r_1 = 0.5$, $r_2 = 0.5$, $\rho = 30$ dB).

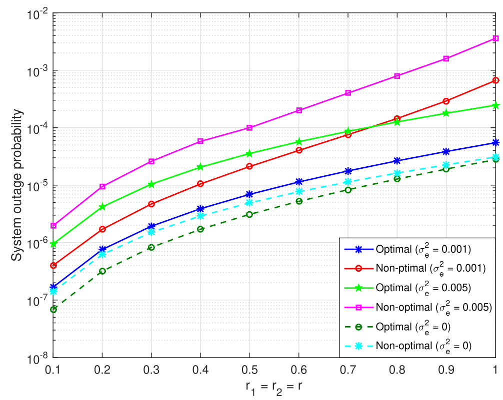

FIGURE 17. System outage probability of NOMA-FD-CDRT network v/s $r_1 = r_2 = r$: optimal and non-optimal.

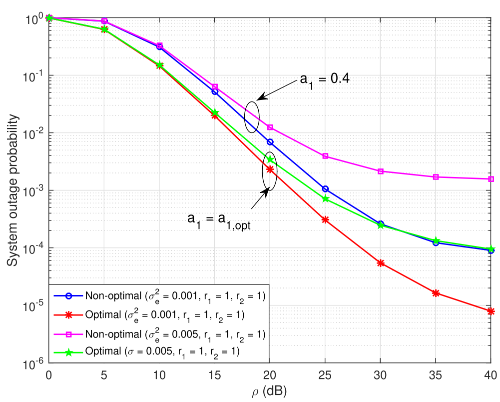

FIGURE 16. System outage probability of NOMA-FD-CDRT network v/s ρ optimal and non-optimal ($r_1 = 1$, $r_2 = 1$).

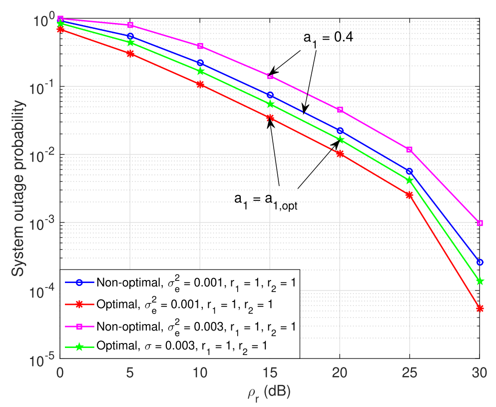

FIGURE 18. System outage probability of NOMA-FD-CDRT network v/s ρ_r: optimal and non-optimal ($\rho_s = 30$ *dB*).

r_1 fixed), $a_{1,opt}^{FD/HD}$ shall be reduced (i.e., $a_{2,opt}^{FD/HD}$ shall be increased). FIGURE 16 and FIGURE 17 show $P_{out,sys}^{FD}$ for optimal/non-optimal cases, where the non-optimal values for $P_{out,sys}^{FD}$ are obtained by setting arbitrary values for a_1 (we call this as random power allocation). From FIGURE 16, $P_{out,sys}^{FD}$ improves by 78% over the non-optimal case ($a_1 = 0.4$, $\rho =$ 30 dB, $\sigma_e^2 = 0.001$, $r_1 = r_2 = 1$). With the proposed $a_{1,opt}^{FD}$, the improvement in $P_{out,sys}^{FD}$ is found to be higher under I-CSI as compared to P-CSI, as can be seen in FIGURE 17. In the above investigations (i.e., FIGURES 14-17), we have kept $\rho_s = \rho_r = \rho$. In FIGURE 18, we set $\rho_s = 30$ *dB* and choose distinct values for ρ_r. The system outage is determined for distinct values of ρ_r. It is observed that increase of ρ_r reduces the system outage for both optimal as well as non-optimal cases. At the same time, the analytical and simulation results shows that $a_{1,opt}^{HD/FD}$ does not depend on ρ_r. This is evident from (44) as well as (52). Overall, our investigations have revealed that $P_{out,sys}^{FD}$ can be minimized by setting $a_1 = a_{1,opt}^{FD/HD}$ in NOMA-FD/HD-CDRT system.

VII. CONCLUSION

The objective of this paper was to investigate the application of NOMA in a coordinated direct and relay transmission (CDRT) system, where the BS serves two geographically separated users, i.e., a near user and a far (cell edge) user, over the downlink; the far user being served with the assistance of a dedicated FD relay node. Realistic assumptions of imperfect channel state information (I-CSI) and imperfect successive interference cancellation (I-SIC) were taken into account for the investigations. Exact closed-form expressions for the outage probability and approximate closed-form expressions for the ergodic rates of the users were derived, under the influence of I-CSI and I-SIC. Extensive simulations were conducted to validate the accuracy of analytical results. The performance gains of the considered NOMA-FD-CDRT system were illustrated by comparing against NOMA-HD-CDRT system and conventional OMA system. Further, analytical expressions for the optimal power allocation (OPA) coefficient at the BS that minimizes the system outage probability of NOMA-FD/HD-CDRT were derived, considering I-CSI. Through extensive numerical and simulation investigations, it was established that selection of OPA coefficient according to the criterion given in the paper can significantly improve the system outage performance of the considered NOMA-FD/HD-CDRT network.

APPENDIXES

APPENDIX A

(i) Derivation of (17) and (18):

Substituting the expressions for Γ_{12}^{FD} and Γ_{11}^{FD} in the definition for $P_{out,1}^{FD}$ in (16),

$$\begin{aligned}
&P_{out,1}^{FD}\\
&= 1 - P_r\left\{\frac{|\hat{h}_{s1}|^2\rho_s a_2}{|\hat{h}_{s1}|^2\rho_s a_1 + |\hat{h}_{r1}|^2\rho_r + \delta_3} \geq u_2^{FD};\right.\\
&\qquad \left.\frac{|\hat{h}_{s1}|^2\rho_s a_1}{\beta a_2\rho_s|\hat{h}_{s1}|^2 + |\hat{h}_{r1}|^2\rho_r + \delta_4} \geq u_1^{FD}\right\}\\
&= 1 - P_r\{|\hat{h}_{s1}|^2\rho_s(a_2 - u_2^{FD}a_1) \geq u_2^{FD}(|\hat{h}_{r1}|^2\rho_r + \delta_3);\\
&\qquad |\hat{h}_{s1}|^2\rho_s(a_1 - \beta u_1^{FD}a_2) \geq u_1^{FD}(|\hat{h}_{r1}|^2\rho_r + \delta_4)\}\\
&= 1 - P_r\left\{|\hat{h}_{s1}|^2\rho_s \geq \frac{u_2^{FD}}{(a_2 - u_2^{FD}a_1)}(|\hat{h}_{r1}|^2\rho_r + \delta_3);\right.\\
&\qquad \left.|\hat{h}_{s1}|^2\rho_s \geq \frac{u_1^{FD}}{(a_1 - \beta u_1^{FD}a_2)}(|\hat{h}_{r1}|^2\rho_r + \delta_4)\right\}\\
&= 1 - \left\{P_r\left\{|\hat{h}_{s1}|^2 \geq \alpha_1|\hat{h}_{r1}|^2 + \beta_1;\ |\hat{h}_{r1}|^2 < \frac{\beta_1 - \beta_2}{\alpha_2 - \alpha_1}\right\}\right.\\
&\qquad \left.+ P_r\left\{|\hat{h}_{s1}|^2 \geq \alpha_2|\hat{h}_{r1}|^2 + \beta_2;\ |\hat{h}_{r1}|^2 > \frac{\beta_1 - \beta_2}{\alpha_2 - \alpha_1}\right\}\right\}\\
&\triangleq 1 - (Z_0 + Z_1)
\end{aligned} \tag{53}$$

where $\alpha_1 = \frac{u_2^{FD}\rho_r}{\rho_s(a_2 - u_2^{FD}a_1)}$, $\beta_1 = \frac{u_2^{FD}\delta_3}{\rho_s(a_2 - u_2^{FD}a_1)}$, $\alpha_2 = \frac{u_1^{FD}\rho_r}{\rho_s(a_1 - \beta u_1^{FD}a_2)}$ and $\beta_2 = \frac{u_1^{FD}\delta_4}{\rho_s(a_1 - \beta u_1^{FD}a_2)}$. To determine Z_0 and Z_1 in (53), we use the expressions for the PDF and the CDF of $|h_{ij}|^2$ given in (2) and (3) respectively. Further, we assume $u_2^{FD} < \frac{a_2}{a_1}$, $u_1^{FD} < \frac{a_1}{a_2\beta}$, $\beta_1 > \beta_2$ and $\alpha_2 > \alpha_1$. Thus Z_0 and Z_1 are obtained as follows:

$$\begin{aligned}
Z_0 &= P_r\left\{|\hat{h}_{s1}|^2 \geq \alpha_1|h_{r1}|^2 + \beta_1;\ |\hat{h}_{r1}|^2 < \frac{\beta_1 - \beta_2}{\alpha_2 - \alpha_1}\right\}\\
&= \int_{x=0}^{\frac{\beta_1-\beta_2}{\alpha_2-\alpha_1}} e^{-\frac{\alpha_1 x+\beta_1}{\hat{\beta}_{s1}}} \sum_{k=0}^{\hat{m}_{s1}-1}\frac{1}{k!}\left(\frac{\alpha_1 x + \beta_1}{\hat{\beta}_{s1}}\right)^k f_{|\hat{h}_{r1}|^2}(x)\,dx\\
&= \int_{x=0}^{\frac{\beta_1-\beta_2}{\alpha_2-\alpha_1}} e^{-\frac{\alpha_1 x+\beta_1}{\hat{\beta}_{s1}}} \sum_{k=0}^{\hat{m}_{s1}-1}\frac{1}{k!}\left(\frac{\alpha_1 x + \beta_1}{\hat{\beta}_{s1}}\right)^k \frac{(k_1\hat{\beta}_{r1})^{-\hat{m}_{r1}}}{\Gamma(\hat{m}_{r1})}\\
&\quad \times e^{-\frac{x}{k_1\hat{\beta}_{r1}}} x^{\hat{m}_{r1}-1}dx\\
&= e^{-\frac{\beta_1}{\hat{\beta}_{s1}}} \sum_{k=0}^{\hat{m}_{s1}-1}\frac{1}{k!}\left(\frac{1}{\hat{\beta}_{s1}}\right)^k \frac{(k_1\hat{\beta}_{r1})^{-\hat{m}_{r1}}}{\Gamma(\hat{m}_{r1})}\\
&\quad \times \int_{x=0}^{\frac{\beta_1-\beta_2}{\alpha_2-\alpha_1}} e^{-\frac{\alpha_1}{\hat{\beta}_{s1}}x}(\alpha_1 x + \beta_1)^k e^{-\frac{x}{k_1\hat{\beta}_{r1}}} x^{\hat{m}_{r1}-1}dx
\end{aligned} \tag{54}$$

Invoking Binomial expansion of the term $(x + \frac{\beta_1}{\alpha_1})^k$ in (54), we get

$$\begin{aligned}
Z_0 &= e^{-\frac{\beta_1}{\hat{\beta}_{s1}}} \sum_{k=0}^{\hat{m}_{s1}-1}\frac{1}{k!}\left(\frac{\alpha_1}{\hat{\beta}_{s1}}\right)^k \frac{(k_1\hat{\beta}_{r1})^{-\hat{m}_{r1}}}{\Gamma(\hat{m}_{r1})} \sum_{j=0}^{k} {}^kC_j\\
&\quad \times \left(\frac{\beta_1}{\alpha_1}\right)^{k-j} \int_{x=0}^{\frac{\beta_1-\beta_2}{\alpha_2-\alpha_1}} e^{-\left(\frac{\alpha_1}{\hat{\beta}_{s1}}+\frac{1}{k_1\hat{\beta}_{r1}}\right)x} x^{j+\hat{m}_{r1}-1}dx
\end{aligned} \tag{55}$$

To evaluate the integral in (55), we use the result from [42] (3.351.1). Accordingly, we get the following expression for Z_0:

$$\begin{aligned}
Z_0 &= e^{-\frac{\beta_1}{\hat{\beta}_{s1}}} \sum_{k=0}^{\hat{m}_{s1}-1}\frac{1}{k!}\left(\frac{\alpha_1}{\hat{\beta}_{s1}}\right)^k \frac{(k_1\hat{\beta}_{r1})^{-\hat{m}_{r1}}}{\Gamma(\hat{m}_{r1})} \sum_{j=0}^{k} {}^kC_j\\
&\quad \times \left(\frac{\beta_1}{\alpha_1}\right)^{k-j} \left(\frac{\alpha_1}{\hat{\beta}_{s1}} + \frac{1}{k_1\hat{\beta}_{r1}}\right)^{-j-\hat{m}_{r1}}\\
&\quad \times \gamma\left(j + \hat{m}_{r1}, \left(\frac{\alpha_1}{\hat{\beta}_{s1}} + \frac{1}{k_1\hat{\beta}_{r1}}\right)\left(\frac{\beta_1 - \beta_2}{\alpha_2 - \alpha_1}\right)\right)
\end{aligned} \tag{56}$$

In (56), $\gamma(.,.)$ is the lower incomplete Gamma function [42]. Notice that Z_1 in (53) is similar to Z_0. Following the approach used for the evaluation of Z_0, Z_1 can be obtained as follows:

$$\begin{aligned}
Z_1 &= e^{-\frac{\beta_2}{\hat{\beta}_{s1}}} \sum_{l=0}^{\hat{m}_{s1}-1}\frac{1}{l!}\left(\frac{\alpha_2}{\hat{\beta}_{s1}}\right)^l \frac{(k_1\hat{\beta}_{r1})^{-\hat{m}_{r1}}}{\Gamma(\hat{m}_{r1})} \sum_{i=0}^{l} {}^lC_i\\
&\quad \times \left(\frac{\beta_2}{\alpha_2}\right)^{l-i} \left(\frac{\alpha_2}{\hat{\beta}_{s1}} + \frac{1}{k_1\hat{\beta}_{r1}}\right)^{-i-\hat{m}_{r1}}\\
&\quad \times \Gamma\left(i + \hat{m}_{r1}, \left(\frac{\alpha_2}{\hat{\beta}_{s1}} + \frac{1}{k_1\hat{\beta}_{r1}}\right)\left(\frac{\beta_1 - \beta_2}{\alpha_2 - \alpha_1}\right)\right)
\end{aligned} \tag{57}$$

In (57), $\Gamma(.,.)$ is the upper incomplete Gamma function [42]. By combining (56) and (57) and substituting in (53), we will get (17). In the absence of residual interference at U_1 (i.e., when $k_1 = 0$), the outage probability of user 1, i.e., $P_{out,1}^{FD}$ can be derived as follows:

$$\begin{aligned}
P_{out,1}^{FD} &= 1 - P_r\left\{\frac{|\hat{h}_{s1}|^2\rho_s a_2}{|\hat{h}_{s1}|^2\rho_s a_1 + \delta_3} \geq u_2^{FD};\right.\\
&\qquad \left.\frac{|\hat{h}_{s1}|^2\rho_s a_1}{\beta a_2\rho_s|\hat{h}_{s1}|^2 + \delta_4} \geq u_1^{FD}\right\}\\
&= 1 - P_r\{|\hat{h}_{s1}|^2\rho_s(a_2 - u_2^{FD}a_1) \geq u_2^{FD}\delta_3;\\
&\qquad |\hat{h}_{s1}|^2\rho_s(a_1 - \beta u_1^{FD}a_2) \geq u_1^{FD}\delta_4\}
\end{aligned} \tag{58a}$$

$$= 1 - P_r\left\{|\hat{h}_{s1}|^2\rho_s \geq \frac{u_2^{FD}\delta_3}{(a_2 - u_2^{FD}a_1)};\ |\hat{h}_{s1}|^2\rho_s \geq \frac{u_1^{FD}\delta_4}{(a_1 - \beta u_1^{FD}a_2)}\right\}$$

$$= 1 - P_r\left\{|\hat{h}_{s1}|^2 \geq \frac{1}{\phi^{FD}\rho_s}\right\} \tag{58b}$$

where $\phi^{FD} = \min\left\{\frac{a_2 - u_2^{FD}a_1}{u_2^{FD}\delta_3}, \frac{a_1 - \beta a_2\, u_1^{FD}}{u_1^{FD}\delta_4}\right\}$. Assume that $u_2^{FD} < \frac{a_2}{a_1}$ and $u_1^{FD} < \frac{a_1}{\beta a_2}$. From (3), $P_r(|\hat{h}_{s1}|^2 \geq x) = e^{-\frac{x}{\hat{\beta}_{s1}}}\sum_{j=0}^{\hat{m}_{s1}-1}\frac{(\frac{x}{\hat{\beta}_{s1}})^j}{j!}$. Substituting this relation in (58b) and after effecting suitable change of variables, $P_{out,1}^{FD}$ is obtained as in (18). From (58a), it is apparent that, when either $u_2^{FD} \geq \frac{a_2}{a_1}$ or $u_1^{FD} \geq \frac{a_1}{\beta a_2}$, $P_{out,1}^{FD}$ becomes unity.

(ii) Derivation of (19) and (20):

To derive (19), we start from (53). For non-integer values of $\hat{m}_{ij}$, Z_0 and Z_1 are determined as follows:

$$Z_0 = P_r\left\{|\hat{h}_{s1}|^2 \geq \alpha_1|\hat{h}_{r1}|^2 + \beta_1;\ |\hat{h}_{r1}|^2 < \frac{\beta_1 - \beta_2}{\alpha_2 - \alpha_1}\right\}$$

$$= \int_{x=0}^{\frac{\beta_1-\beta_2}{\alpha_2-\alpha_1}}\left(1 - \sum_{g=0}^{\infty}\frac{1}{\Gamma(\hat{m}_{s1}+g+1)}e^{-\frac{(\alpha_1 x+\beta_1)}{\hat{\beta}_{s1}}}\times\left(\frac{(\alpha_1 x+\beta_1)}{\hat{\beta}_{s1}}\right)^{\hat{m}_{s1}+g}\right)\frac{(k_1\hat{\beta_{r1}})^{-\hat{m}_{r1}}}{\Gamma(\hat{m}_{r1})}e^{-\frac{x}{k_1\hat{\beta}_{r1}}}x^{\hat{m}_{r1}-1}dx$$

$$= \frac{(k_1\hat{\beta_{r1}})^{-\hat{m}_{r1}}}{\Gamma(\hat{m}_{r1})}\int_{x=0}^{\frac{\beta_1-\beta_2}{\alpha_2-\alpha_1}}e^{-\frac{x}{k_1\hat{\beta}_{r1}}}x^{\hat{m}_{r1}-1}dx - \frac{(k_1\hat{\beta_{r1}})^{-\hat{m}_{r1}}}{\Gamma(\hat{m}_{r1})}\sum_{g=0}^{\infty}\frac{1}{\Gamma(\hat{m}_{s1}+g+1)}\left(\frac{1}{\hat{\beta}_{s1}}\right)^{\hat{m}_{s1}+g}e^{-\frac{\beta_1}{\hat{\beta}_{s1}}}\times\int_{x=0}^{\frac{\beta_1-\beta_2}{\alpha_2-\alpha_1}}e^{-\left(\frac{\alpha_1}{\hat{\beta}_{s1}}+\frac{1}{k_1\hat{\beta}_{r1}}\right)x}(\alpha_1 x+\beta_1)^{\hat{m}_{s1}+g}x^{\hat{m}_{r1}-1}dx \tag{59}$$

Using Binomial expansion for the term $(1+\frac{\beta_1}{\alpha_1\, x})^{\hat{m}_{s1}+g}$ for non integer values of $(\hat{m}_{s1}+g)$ in (59), we get

$$Z_0 = \frac{(k_1\hat{\beta_{r1}})^{-\hat{m}_{r1}}}{\Gamma(\hat{m}_{r1})}\frac{\gamma(\hat{m}_{r1}, (\frac{1}{k_1\hat{\beta}_{r1}})(\frac{\beta_1-\beta_2}{\alpha_2-\alpha_1}))}{(\frac{1}{k_1\hat{\beta}_{r1}})^{\hat{m}_{r1}}} - \frac{(k_1\hat{\beta_{r1}})^{-\hat{m}_{r1}}}{\Gamma(\hat{m}_{r1})}\sum_{g=0}^{\infty}\frac{1}{\Gamma(\hat{m}_{s1}+g+1)}\left(\frac{1}{\hat{\beta}_{s1}}\right)^{\hat{m}_{s1}+g}e^{-\frac{\beta_1}{\hat{\beta}_{s1}}}\times\sum_{k=0}^{\infty}{}^{\hat{m}_{s1}+g}C_k\left(\frac{\beta_1}{\alpha_1}\right)^k\alpha_1^{\hat{m}_{s1}+g}\int_{x=0}^{\frac{\beta_1-\beta_2}{\alpha_2-\alpha_1}}e^{-\left(\frac{\alpha_1}{\hat{\beta}_{s1}}+\frac{1}{k_1\hat{\beta}_{r1}}\right)x}\times x^{\hat{m}_{s1}+\hat{m}_{r1}+g-k-1}dx$$

$$= \frac{\gamma(\hat{m}_{r1}, (\frac{1}{k_1\hat{\beta}_{r1}})(\frac{\beta_1-\beta_2}{\alpha_2-\alpha_1}))}{\Gamma(\hat{m}_{r1})} - \frac{(k_1\hat{\beta_{r1}})^{-\hat{m}_{r1}}}{\Gamma(\hat{m}_{r1})}\sum_{g=0}^{\infty}\frac{1}{\Gamma(\hat{m}_{s1}+g+1)}\left(\frac{1}{\hat{\beta}_{s1}}\right)^{\hat{m}_{s1}+g}e^{-\frac{\beta_1}{\hat{\beta}_{s1}}}\times\sum_{k=0}^{\infty}{}^{\hat{m}_{s1}+g}C_k\left(\frac{\beta_1}{\alpha_1}\right)^k\alpha_1^{\hat{m}_{s1}+g}\times\frac{\gamma\left(\hat{m}_{s1}+\hat{m}_{r1}+g-k, (\frac{\alpha_1}{\hat{\beta}_{s1}}+\frac{1}{k_1\hat{\beta}_{r1}})\right)\frac{\beta_1-\beta_2}{\alpha_2-\alpha_1}}{(\frac{\alpha_1}{\hat{\beta}_{s1}}+\frac{1}{k_1\hat{\beta}_{r1}})^{\hat{m}_{s1}+\hat{m}_{r1}+g-k}} \tag{60}$$

For non-integer values of $\hat{m}_{ij}$, the quantity Z_0 in (53) can be determined by following a similar approach. Thus Z_1 is given by

$$Z_1 = \frac{\Gamma(\hat{m}_{r1}, (\frac{1}{k_1\hat{\beta}_{r1}})(\frac{\beta_1-\beta_2}{\alpha_2-\alpha_1}))}{\Gamma(\hat{m}_{r1})} - \frac{(k_1\hat{\beta_{r1}})^{-\hat{m}_{r1}}}{\Gamma(\hat{m}_{r1})}\sum_{i=0}^{\infty}\frac{1}{\Gamma(\hat{m}_{s1}+i+1)}\left(\frac{1}{\hat{\beta}_{s1}}\right)^{\hat{m}_{s1}+i}e^{-\frac{\beta_1}{\hat{\beta}_{s1}}}\times\sum_{l=0}^{\infty}{}^{\hat{m}_{s1}+i}C_l\left(\frac{\beta_1}{\alpha_1}\right)^l\alpha_1^{\hat{m}_{s1}+i}\frac{\Gamma\left(\hat{m}_{s1}+\hat{m}_{r1}+i-l, (\frac{\alpha_1}{\hat{\beta}_{s1}}+\frac{1}{k_1\hat{\beta}_{r1}})\right)\frac{\beta_1-\beta_2}{\alpha_2-\alpha_1}}{(\frac{\alpha_1}{\hat{\beta}_{s1}}+\frac{1}{k_1\hat{\beta}_{r1}})^{\hat{m}_{s1}+\hat{m}_{r1}+i-l}} \tag{61}$$

Combining (60) and (61) and substituting in (53), we will get (19). In the absence of residual interference at U_1 (i.e., when $k_1 = 0$) and non-integer values of m, the outage probability of user 1 can be derived from (58b) and is given by

$$P_{out,1}^{FD} = 1 - P_r\left\{|\hat{h}_{s1}|^2 \geq \frac{1}{\phi^{FD}\rho_s}\right\} = 1 - e^{-\frac{1}{\phi^{FD}\rho_s\hat{\beta}_{s1}}}\sum_{g=0}^{\infty}\frac{1}{\Gamma(\hat{m}_{s1}+g+1)}\times\left(\frac{1}{\phi^{FD}\rho_s\hat{\beta}_{s1}}\right)^{\hat{m}_{s1}+g} \tag{62}$$

Propositions 1(a) and 1(b) are thus proved.

APPENDIX B

(i) Derivation of (24):

Substituting the expression for Γ_{r2}^{FD} and Γ_{22}^{FD} in the definition for $P_{out,2}^{FD}$ in (23), we get

$$P_{out,2}^{FD} = 1 - P_r\left\{\frac{|\hat{h}_{sr}|^2\rho_s a_2}{|\hat{h_{sr}}|^2\rho_s a_1 + |h_{rr}|^2\rho_r + \delta_1} \geq u_2^{FD};\ \frac{|\hat{h}_{r2}|^2\rho_r}{\delta_2} \geq u_2^{FD}\right\} \tag{63a}$$

$$= 1 - P_r\left\{|\hat{h}_{sr}|^2\rho_s(a_2 - u_2^{FD}a_1) \geq u_2^{FD}(|h_{rr}|^2\rho_r + \delta_1);\ |\hat{h}_{r2}|^2 \geq \frac{u_2^{FD}\delta_2}{\rho_r}\right\} \tag{63b}$$

$$= 1 - P_r\left\{|\hat{h}_{sr}|^2 \geq \frac{1}{\rho_s \psi^{FD}}(|h_{rr}|^2\rho_r + \delta_1)\right\} \times P_r\left\{|\hat{h}_{r2}|^2 \geq \frac{u_2^{FD}\delta_2}{\rho_r}\right\} \tag{63c}$$

$$\triangleq 1 - (X_0 \times Y_0) \tag{63d}$$

were $\psi^{FD} = \frac{a_2 - u_2^{FD}a_1}{u_2^{FD}}$. Here (63c) follows since $|\hat{h}_{sr}^2|$ and $|\hat{h}_{r2}^2|$ are assumed to be independent. Further, $|\hat{h}_{sr}|^2 \sim Gamma(\hat{m}_{sr}, \hat{\pi}_{sr})$ and $|\hat{h}_{r2}|^2 \sim Gamma(\hat{m}_{r2}, \hat{\pi}_{r2})$. For integer values of $\hat{m}_{sr}$ and $\hat{m}_{r2}$, $P_r(|\hat{h}_{sr}|^2 \geq x) = e^{-\frac{x}{\hat{\beta}_{sr}}}\sum_{j=0}^{\hat{m}_{sr}-1}\frac{(\frac{x}{\hat{\beta}_{sr}})^j}{j!}$ and $P_r(|\hat{h}_{r2}|^2 \geq y) = e^{-\frac{y}{\hat{\beta}_{r2}}}\sum_{k=0}^{\hat{m}_{r2}-1}\frac{(\frac{y}{\hat{\beta}_{r2}})^k}{k!}$. Thus X_0 and Y_0 in (63d) are determined as follows:

$$X_0 = P_r\left\{|\hat{h}_{sr}|^2 \geq \frac{1}{\rho_s\psi^{FD}}(|h_{rr}|^2\rho_r + \delta_1)\right\}$$

$$= \int_{y=0}^{\infty} e^{-\frac{1}{\rho_s\psi^{FD}\hat{\beta}_{sr}}(y\rho_r+\delta_1)} \sum_{j=0}^{\hat{m}_{sr}-1}\frac{1}{j!}\left(\frac{y\rho_r+\delta_1}{\psi^{FD}\rho_s\hat{\beta}_{sr}}\right)^j \times f_{|h_{rr}|^2}(y)dy$$

$$= \int_0^{\infty} e^{-(\frac{y\rho_r+\delta_1}{\psi^{FD}\rho_s\hat{\beta}_{sr}})}\sum_{j=0}^{\hat{m}_{sr}-1}\frac{1}{j!}\left(\frac{y\rho_r+\delta_1}{\psi^{FD}\rho_s\hat{\beta}_{sr}}\right)^j \times (k_2\beta_{rr})^{-m_{rr}}\frac{y^{m_{rr}-1}}{\Gamma(m_{rr})}e^{-\frac{y}{\beta_{rr}k_2}}dy$$

$$= e^{-\frac{\delta_1}{\psi^{FD}\rho_s\hat{\beta}_{sr}}}\frac{(k_2\beta_{rr})^{-m_{rr}}}{\Gamma(m_{rr})}\sum_{j=0}^{\hat{m}_{sr}-1}\frac{1}{j!}\left(\frac{\rho_r}{\psi^{FD}\rho_s\hat{\beta}_{sr}}\right)^j \times\int_{y=0}^{\infty}(y+\delta_1/\rho_r)^j y^{m_{rr}-1}e^{-(\frac{\rho_r}{\psi^{FD}\rho_s\hat{\beta}_{sr}}+\frac{1}{k_2\beta_{rr}})y}dy \tag{64a}$$

By using Binomial expansion of the term $(y+\frac{\delta_1}{\rho_r})^j$, (64a) can be written as follows:

$$X_0 = e^{-\frac{\delta_1}{\psi^{FD}\rho_s\hat{\beta}_{sr}}}\frac{(k_2\beta_{rr})^{-m_{rr}}}{\Gamma(m_{rr})}\sum_{j=0}^{\hat{m}_{sr}-1}\frac{1}{j!}\left(\frac{\rho_r}{\psi^{FD}\rho_s\hat{\beta}_{sr}}\right)^j \times\sum_{l=0}^{j}{}^jC_l\left(\frac{\delta_1}{\rho_r}\right)^{j-l} \times\int_{y=0}^{\infty}\left[y^{l+m_{rr}-1}\times e^{-(\frac{\rho_r}{\psi^{FD}\rho_s\hat{\beta}_{sr}}+\frac{1}{k_2\beta_{rr}})y}\right]dy \tag{64b}$$

To simplify (64b), we use the following result from [42] (3.351.3):

$$\int_0^{\infty}x^n e^{-\mu x}dx = n!\mu^{-n-1} \tag{65}$$

Thus the final expression for X_0 is given by:

$$X_0 = e^{-\frac{\delta_1}{\rho_s\psi^{FD}\hat{\beta}_{sr}}}\frac{(k_2\beta_{rr})^{-m_{rr}}}{\Gamma(m_{rr})}\sum_{j=0}^{\hat{m}_{sr}-1}\left(\frac{\rho_r}{\rho_s\psi^{FD}\hat{\beta}_{sr}}\right)^j \times\sum_{l=0}^{j}{}^jC_l\left(\frac{\delta_1}{\rho_r}\right)^{j-l}(l+m_{rr}-1)! \times\left(\frac{\rho_r}{\rho_s\psi^{FD}\hat{\beta}_{sr}}+\frac{1}{k_2\beta_{rr}}\right)^{-l-m_{rr}} \tag{66}$$

Next Y_0 is determined as follows:

$$Y_0 = P_r\left\{|\hat{h}_{r2}|^2 \geq \frac{u_2^{FD}\delta_2}{\rho_r}\right\} = e^{-\frac{u_2^{FD}\delta_2}{\rho_r\hat{\beta}_{r2}}}\sum_{i=0}^{\hat{m}_{r2}-1}\frac{1}{i!}\left(\frac{u_2^{FD}\delta_2}{\rho_r\hat{\beta}_{r2}}\right)^i \tag{67}$$

Using (66) and (67) in (63d), we get the final expression for $P_{out,2}^{FD}$ as given in (24). Notice that (24) is valid if and only if $u_2^{FD} < \frac{a_2}{a_1}$. From (63b), it is clear that if $u_2^{FD} \geq \frac{a_2}{a_1}$, the probability term on the RHS of (63b) becomes zero, which makes $P_{out,2}^{FD}$ equal to unity.

(ii) Derivation of (25):

To derive (25), we start from (63d). For non-integer values of $\hat{m}_{ij}$, X_0 and Y_0 are determined as follows:

$$X_0 = P_r\left\{|\hat{h}_{sr}|^2 \geq \frac{1}{\rho_s\psi^{FD}}(|h_{rr}|^2\rho_r + \delta_1)\right\}$$

$$= \int_{x=0}^{\infty}\left(1 - \sum_{h=0}^{\infty}\frac{1}{\Gamma(\hat{m}_{sr}+h+1)}e^{-\frac{(x\rho_r+\delta_1)}{\rho_s\psi^{FD}\hat{\beta}_{sr}}} \times\left(\frac{(x\rho_r+\delta_1)}{\rho_s\psi^{FD}\hat{\beta}_{sr}}\right)^{\hat{m}_{sr}+h}\right)\frac{(k_2\hat{\beta}_{rr})^{-\hat{m}_{rr}}}{\Gamma(\hat{m}_{rr})}e^{-\frac{x}{k_2\hat{\beta}_{rr}}}x^{\hat{m}_{rr}-1}dx$$

$$= 1 - \frac{(k_2\hat{\beta}_{rr})^{-\hat{m}_{rr}}}{\Gamma(\hat{m}_{rr})}\sum_{h=0}^{\infty}\frac{1}{\Gamma(\hat{m}_{sr}+h+1)} \times\left(\frac{1}{\rho_s\psi^{FD}\hat{\beta}_{sr}}\right)^{\hat{m}_{sr}+h}e^{-\frac{\delta_1}{\rho_s\psi^{FD}\hat{\beta}_{sr}}} \times\int_{x=0}^{\infty}\left[e^{-(\frac{\rho_r}{\rho_s\psi^{FD}\hat{\beta}_{sr}}+\frac{1}{k_2\hat{\beta}_{rr}})x}(\rho_r x+\delta_1)^{\hat{m}_{sr}+h}x^{\hat{m}_{rr}-1}\right]dx \tag{68}$$

Using Binomial expansion for the term $(1+\frac{\delta_1}{\rho_r x})^{\hat{m}_{sr}+h}$ for non integer values of $(\hat{m}_{s1}+h)$ in (68), we will get

$$X_0 = 1 - \frac{(k_2\hat{\beta}_{rr})^{-\hat{m}_{rr}}}{\Gamma(\hat{m}_{rr})}\sum_{h=0}^{\infty}\frac{1}{\Gamma(\hat{m}_{sr}+h+1)}\left(\frac{1}{\rho_s\psi^{FD}\hat{\beta}_{sr}}\right)^{\hat{m}_{sr}+h} \times e^{-\frac{\delta_1}{\rho_s\psi^{FD}\hat{\beta}_{sr}}}(\rho_r)^{\hat{m}_{sr}+h}\sum_{k=0}^{\infty}{}^{\hat{m}_{sr}+h}C_k\left(\frac{\delta_1}{\rho_r}\right)^k \times\int_{x=0}^{\infty}e^{-(\frac{\rho_r}{\rho_s\psi^{FD}\hat{\beta}_{sr}}+\frac{1}{k_2\hat{\beta}_{rr}})x}x^{\hat{m}_{sr}+\hat{m}_{rr}+h-k-1}dx$$

$$= 1 - \frac{(k_2\hat{\beta}_{rr})^{-\hat{m}_{rr}}}{\Gamma(\hat{m}_{rr})}\sum_{h=0}^{\infty}\frac{1}{\Gamma(\hat{m}_{sr}+h+1)}\left(\frac{1}{\rho_s\psi^{FD}\hat{\beta}_{sr}}\right)^{\hat{m}_{sr}+h} \times e^{-\frac{\delta_1}{\rho_s\psi^{FD}\hat{\beta}_{sr}}}(\rho_r)^{\hat{m}_{sr}+h}\sum_{k=0}^{\infty}{}^{\hat{m}_{sr}+h}C_k\left(\frac{\delta_1}{\rho_r}\right)^k \times\frac{\Gamma(\hat{m}_{sr}+\hat{m}_{rr}+h-k)}{(\frac{\rho_r}{\rho_s\psi^{FD}\hat{\beta}_{sr}}+\frac{1}{k_2\hat{\beta}_{rr}})^{\hat{m}_{sr}+\hat{m}_{rr}+h-k}} \tag{69}$$

For non-integer values of m_{ij}, Y_0 in (63d) can be determined by using (3) as follows:

$$Y_0 = P_r\left\{|\hat{h}_{r2}|^2 \geq \frac{u_2^{FD}\delta_2}{\rho_r}\right\} = 1 - e^{-\frac{u_2^{FD}\delta_2}{\rho_r\hat{\beta}_{r2}}}\sum_{g=0}^{\infty}\frac{1}{\Gamma(\hat{m}_{r2}+g+1)}\left(\frac{u_2^{FD}\delta_2}{\rho_r\hat{\beta}_{r2}}\right)^{\hat{m}_{r2}+g} \tag{70}$$

Substituting (69) and (70) in (63d) gives (25). The propositions 2(a) and 2(b) are thus proved.

APPENDIX C

(i) Derivation of (29) and (30)

Substituting the expressions for Γ_{11}^{FD}, Γ_{12}^{FD}, Γ_{r2}^{FD} and Γ_{22}^{FD} in (28), $P_{out,sys}^{FD}$ becomes:

$$\begin{aligned} P_{out,sys}^{FD} &= 1 - P_r\Bigg\{\frac{|\hat{h}_{s1}|^2\rho_s a_2}{|\hat{h}_{s1}|^2\rho_s a_1 + |\hat{h}_{r1}|^2\rho_r + \delta_3} \geq u_2^{FD}; \\ &\quad \frac{|\hat{h}_{s1}|^2\rho_s a_1}{\beta a_2\rho_s|\hat{h}_{s1}|^2 + |\hat{h}_{r1}|^2\rho_r + \delta_4} \geq u_1^{FD}, \\ &\quad \frac{|\hat{h}_{sr}|^2\rho_s a_2}{|\hat{h_{sr}}|^2\rho_s a_1 + |h_{rr}|^2\rho_r + \delta_1} \geq u_2^{FD}, \frac{|\hat{h}_{r2}|^2\rho_r}{\delta_2} \geq u_2^{FD}\Bigg\} \end{aligned} \tag{71a}$$

$$\begin{aligned} &= 1 - P_r\Big\{|\hat{h}_{s1}|^2\rho_s(a_2 - u_2^{FD}a_1) \geq u_2^{FD}(|\hat{h}_{r1}|^2\rho_r + \delta_3); \\ &\quad |\hat{h}_{s1}|^2\rho_s(a_1 - \beta u_1^{FD}a_2) \geq u_1^{FD}(|\hat{h}_{r1}|^2\rho_r + \delta_4); \\ &\quad |\hat{h}_{sr}|^2\rho_s(a_2 - u_2^{FD}a_1) \geq u_2^{FD}(|h_{rr}|^2\rho_r + \delta_1), \\ &\quad |\hat{h}_{r2}|^2\rho_r \geq u_2^{FD}\delta_2\Big\} \end{aligned} \tag{71b}$$

$$\begin{aligned} &= 1 - \Bigg[\Bigg\{P_r\Big\{|\hat{h}_{s1}|^2 \geq \alpha_1|h_{r1}|^2 + \beta_1;\ |\hat{h}_{r1}|^2 < \frac{\beta_1-\beta_2}{\alpha_2-\alpha_1}\Big\} \\ &\quad + P_r\Big\{|\hat{h}_{s1}|^2 \geq \alpha_2|h_{r1}|^2 + \beta_2;\ |\hat{h}_{r1}|^2 > \frac{\beta_1-\beta_2}{\alpha_2-\alpha_1}\Big\}\Bigg\} \\ &\quad \times\Bigg[P_r\Big\{|\hat{h}_{sr}|^2 \geq \frac{1}{\rho_s\psi^{FD}}(|h_{rr}|^2\rho_r + \delta_1)\Big\} \\ &\quad \times P_r\Big\{|\hat{h}_{r2}|^2 \geq \frac{u_2^{FD}\delta_2}{\rho_r}\Big\}\Bigg]\Bigg] \end{aligned} \tag{71c}$$

where β_1, β_2, α_1, α_2 and ψ^{FD} were defined earlier. Under i.n.i.d fading, $P_{out,sys}^{FD}$ becomes

$$P_{out,sys}^{FD} \triangleq 1 - [(E_0 + F_0) \times G_0 \times H_0] \tag{71d}$$

where the quantities E_0 and F_0 are equivalent to Z_0 and Z_1 respectively in Appendix A; further the quantities G_0 and H_0 are equivalent to X_0 and Y_0 respectively in Appendix B. Here $u_2^{FD} < \frac{a_2}{a_1}$, $u_1^{FD} < \frac{a_1}{\beta a_2}$, $\beta_1 > \beta_2$ and $\alpha_2 > \alpha_1$. Accordingly, we substitute Z_0 and Z_1 given by (56) and (57) for E_0 and F_0 in (71d). Further, we substitute X_0 and Y_0 given by (66) and (67) for G_0 and H_0 in (71d). Thus $P_{out,sys}^{FD}$ given by (29) can be obtained.

In the absence of residual interference at U_1 from R (i.e., $k_1 = 0$), $P_{out,sys}^{FD}$ can be determined as follows: when $k_1 = 0$, $|h_{r1}|^2\rho_r$ term will be absent in the expressions for Γ_{11}^{FD} and Γ_{12}^{FD}. Accordingly, $P_{out,sys}^{FD}$ becomes:

$$\begin{aligned} P_{out,sys}^{FD} &= 1 - P_r\Bigg\{\frac{|\hat{h}_{s1}|^2\rho_s a_2}{|\hat{h}_{s1}|^2\rho_s a_1 + \delta_3} \geq u_2^{FD}, \\ &\quad \frac{|\hat{h}_{s1}|^2\rho_s a_1}{\beta a_2\rho_s|\hat{h}_{s1}|^2 + \delta_4} \geq u_1^{FD}, \\ &\quad \frac{|\hat{h}_{sr}|^2\rho_s a_2}{|\hat{h_{sr}}|^2\rho_s a_1 + |h_{rr}|^2\rho_r + \delta_1} \geq u_2^{FD}, \frac{|\hat{h}_{r2}|^2\rho_r}{\delta_2} \geq u_2^{FD}\Bigg\} \end{aligned} \tag{72a}$$

$$\begin{aligned} &= 1 - P_r\Big\{|\hat{h}_{s1}|^2\rho_s(a_2 - u_2^{FD}a_1) \geq u_2^{FD}\delta_3, \\ &\quad |\hat{h}_{s1}|^2\rho_s(a_1 - \beta a_2 u_1^{FD}) \geq u_1^{FD}\delta_4, \\ &\quad |\hat{h}_{sr}|^2\rho_s(a_2 - u_2^{FD}a_1) \geq u_2^{FD}(|h_{rr}|^2\rho_r + \delta_1), \\ &\quad |\hat{h}_{r2}|^2\rho_r \geq u_2^{FD}\delta_2\Big\} \end{aligned} \tag{72b}$$

$$\begin{aligned} &= 1 - P_r\Big\{|\hat{h}_{s1}|^2 \geq \frac{1}{\phi^{FD}\rho_s}; \\ &\quad |\hat{h}_{sr}|^2 \geq \frac{1}{\rho_s\psi^{FD}}(|h_{rr}|^2\rho_r + \delta_1);\ |\hat{h}_{r2}|^2 \geq \frac{u_2^{FD}\delta_2}{\rho_r}\Big\} \end{aligned} \tag{72c}$$

where ϕ^{FD} and ψ^{FD} were defined earlier in Appendix A and Appendix B respectively. Under i.n.i.d fading, $P_{out,sys}^{FD}$ becomes

$$\begin{aligned} P_{out,sys}^{FD} &= 1 - P_r\Big\{|\hat{h}_{s1}|^2 \geq \frac{1}{\phi^{FD}\rho_s}\Big\} \\ &\quad \times P_r\Big\{|\hat{h}_{sr}|^2 \geq \frac{1}{\rho_s\psi^{FD}}(|h_{rr}|^2\rho_r + \delta_1)\Big\} \\ &\quad \times P_r\Big\{|\hat{h}_{r2}|^2 \geq \frac{u_2^{FD}\delta_2}{\rho_r}\Big\} \end{aligned} \tag{72d}$$

$$\triangleq 1 - (A_0 \times B_0 \times C_0) \tag{72e}$$

Here $u_2^{FD} < \frac{a_2}{a_1}$ and $u_1^{FD} < \frac{a_1}{\beta a_2}$. The quantities A_0, B_0 and C_0 are determined as follows: Since $|\hat{h}_{s1}|^2 \sim Gamma(\hat{m}_{s1}, \hat{\pi}_{s1})$, for integer values of $\hat{m}_{s1}$, A_0 is given by:

$$A_0 = e^{-\frac{1}{\phi^{FD}\rho_s\hat{\beta}_{s1}}}\sum_{j=0}^{\hat{m}_{s1}-1}\frac{1}{j!}\left(\frac{1}{\phi^{FD}\rho_s\hat{\beta}_{s1}}\right)^j \tag{73}$$

Now B_0 in (72e) is same as X_0 defined in (63d), thus final expression for B_0 is given by (66), i.e.,

$$\begin{aligned} B_0 &= e^{-\frac{\delta_1}{\rho_s\psi^{FD}\hat{\beta}_{sr}}}\frac{(k_2\beta_{rr})^{-m_{rr}}}{\Gamma(m_{rr})}\sum_{k=0}^{\hat{m}_{sr}-1}\left(\frac{\rho_r}{\rho_s\psi^{FD}\hat{\beta}_{sr}}\right)^k \\ &\quad \times\sum_{l=0}^{k}{}^kC_l\left(\frac{\delta_1}{\rho_r}\right)^{k-l}(l+m_{rr}-1)! \\ &\quad \times\left(\frac{\rho_r}{\rho_s\psi^{FD}\hat{\beta}_{sr}} + \frac{1}{k_2\beta_{rr}}\right)^{-l-m_{rr}} \end{aligned} \tag{74}$$

Finally C_0 is same as Y_0 in (63d) and is given by (67). Thus $P_{out,sys}^{FD}$ is determined by combining (73), (74) and (67) with (72e) and is given by (30). Notice that, when either $u_2^{FD} \geq \frac{a_2}{a_1}$ or $u_1^{FD} \geq \frac{a_1}{a_2\beta}$, the probability term on the RHS of (72c) becomes zero so that $P_{out,sys}^{FD}$ becomes unity. Proposition 3(a) is thus proved.

(ii) Derivation of (31) and (32)

For non-integer values of $\hat{m}_{ij}$, $P_{out,sys}^{FD}$ given by (31) and (32) can be obtained by following the above approach and by utilizing (3). For this, we start with (71d). When $\hat{m}_{ij}$ takes non-integer values, the quantities E_0 and F_0 are derived in Appendix A. These are given by Z_0 and Z_1 in Appendix A in (60) and (61) respectively. Similarly, for non-integer values of $\hat{m}_{ij}$, G_0 and H_0 in (71d) are same as X_0 and Y_0 in Appendix B given by (69) and (70) respectively. Thus utilizing (60), (61), (69) and (70) in (71d), we get (31). The proposition 4 is thus proved.

APPENDIX D
DERIVATION OF (36) AND (37)

To find $E[R_1^{FD}]$ using (35), we need $F_{\Gamma_{11}^{FD}}(x)$, which is determined as follows:

$$\begin{aligned}
&F_{\Gamma_{11}^{FD}}(x)\\
&= 1 - P_r\left(\frac{|\hat{h}_{s1}|^2\rho_s a_1}{\beta a_2\rho_s|\hat{h}_{s1}|^2 + |\hat{h}_{r1}|^2\rho_r + \delta_4} > x\right)\\
&= 1 - P_r\left(|\hat{h}_{s1}|^2 > \frac{x(|\hat{h}_{r1}|^2\rho_r + \delta_4)}{\rho_s(a_1 - x\beta a_2)}\right) \qquad (75)\\
&= 1 - \left[\frac{(k_1\hat{\beta}_{r1})^{-\hat{m}_{r1}}}{\Gamma(\hat{m}_{r1})} e^{-\frac{x\delta_4}{\rho_s(a_1 - xa_2\beta)\hat{\beta}_{s1}}}\right.\\
&\quad \times \sum_{k=0}^{\hat{m}_{s1}-1}\frac{1}{k!}\left(\frac{x\rho_r}{\rho_s(a_1 - xa_2\beta)\hat{\beta}_{s1}}\right)^k\\
&\quad \left.\times \int_{z=0}^{\infty} e^{-\left(\frac{x\rho_r}{\rho_s(a_1 - xa_2\beta)\hat{\beta}_{s1}} + \frac{1}{k_1\hat{\beta}_{r1}}\right)z}(z\rho_r + \delta_4)^j z^{\hat{m}_{r1}-1}dz\right] \qquad (76)
\end{aligned}$$

Notice that (76), is obtained by utilizing the PDF and CDF of $|h_{ij}|^2$ given in (2) and (3). By using Binomial expansion for the term $(z + \frac{\delta_4}{\rho_r})^j$, (76) can be written as,

$$\begin{aligned}
&F_{\Gamma_{11}}^{FD}(x)\\
&= 1 - \left[\frac{(k_1\hat{\beta}_{r1})^{-\hat{m}_{r1}}}{\Gamma(\hat{m}_{r1})} e^{-\frac{x\delta_4}{\rho_s(a_1 - xa_2\beta)\hat{\beta}_{s1}}}\right.\\
&\quad \times \sum_{k=0}^{\hat{m}_{s1}-1}\frac{1}{k!}\left(\frac{x\rho_r}{\rho_s(a_1 - xa_2\beta)\hat{\beta}_{s1}}\right)^k \sum_{i=0}^{k} {}^kC_i\left(\frac{\delta_4}{\rho_r}\right)^{k-i}\\
&\quad \left.\times \int_{z=0}^{\infty} e^{-\left(\frac{x\rho_r}{\rho_s(a_1 - xa_2\beta)\hat{\beta}_{s1}} + \frac{1}{k_1\hat{\beta}_{r1}}\right)z} z^{k+\hat{m}_{r1}-1}dz\right] \qquad (77)
\end{aligned}$$

Using [42] (3.351.3), (77) can be written as

$$\begin{aligned}
&F_{\Gamma_{11}}^{FD}(x)\\
&= 1 - \left[\frac{(k_1\hat{\beta}_{r1})^{-\hat{m}_{r1}}}{\Gamma(\hat{m}_{r1})} e^{-\frac{x\delta_4}{\rho_s(a_1 - xa_2\beta)\hat{\beta}_{s1}}} \sum_{k=0}^{\hat{m}_{s1}-1}\frac{1}{k!}\right.\\
&\quad \times \left(\frac{x\rho_r}{\rho_s(a_1 - xa_2\beta)\hat{\beta}_{s1}}\right)^k \sum_{i=0}^{k} {}^kC_i\left(\frac{\delta_4}{\rho_r}\right)^{k-i}(i + \hat{m}_{r1} - 1)!\\
&\quad \left.\times \left(\frac{x\rho_r}{\rho_s(a_1 - xa_2\beta)\hat{\beta}_{s1}} + \frac{1}{k_1\hat{\beta}_{r1}}\right)^{-k-\hat{m}_{r1}}\right] \qquad (78)
\end{aligned}$$

Substituting (78) in (35), $E[R_1^{FD}]$ is given by

$$\begin{aligned}
&E[R_1^{FD}]\\
&= \frac{1}{ln2}\frac{(k_1\hat{\beta}_{r1})^{-\hat{m}_{r1}}}{\Gamma(\hat{m}_{r1})}\sum_{k=0}^{\hat{m}_{s1}-1}\frac{1}{k!}\sum_{i=0}^{k} {}^kC_i\left(\frac{\delta_4}{\rho_r}\right)^{k-i}(i + \hat{m}_{r1} - 1)!\\
&\quad \times \int_{x=0}^{\frac{a_1}{a_2\beta}} \frac{e^{-\frac{x\delta_4}{\rho_s(a_1 - xa_2\beta)\hat{\beta}_{s1}}}}{1 + x}\left(\frac{x\delta_4}{\rho_s(a_1 - xa_2\beta)\hat{\beta}_{s1}}\right)^k\\
&\quad \times \left(\frac{x\rho_r}{\rho_s(a_1 - xa_2\beta)\hat{\beta}_{s1}} + \frac{1}{k_1\hat{\beta}_{r1}}\right)^{-k-\hat{m}_{r1}} dx \qquad (79)
\end{aligned}$$

Notice that it is challenging to obtain a closed-form expression for $E[R_1^{FD}]$. Hence we use the Gaussian-Chebyshev quadrature [43] to find an approximation for the integral term in (79). The basic approximation relation in Gaussian-Chebyshev quadrature method is given by

$$\int_{-1}^{1}\frac{f(x)}{\sqrt{(1 - x^2)}}dx \approx \frac{\pi}{N}\sum_{n=1}^{N} f\left[cos\left(\frac{(2n - 1)\pi}{2N}\right)\right] \qquad (80)$$

By substituting $x = \frac{1}{2}\frac{a_1}{a_2\beta}(1 + \phi_n)$ and using (80), the integral in (79) becomes,

$$\begin{aligned}
&\int_{x=0}^{\frac{a_1}{a_2\beta}} \frac{e^{-\frac{x\delta_4}{\rho_s(a_1 - xa_2\beta)\hat{\beta}_{s1}}}}{1 + x}\left(\frac{x\delta_4}{\rho_s(a_1 - xa_2\beta)\hat{\beta}_{s1}}\right)^j dx\\
&\qquad\qquad \cong \frac{\pi}{N}\sum_{n=1}^{N}\frac{a_n p_n}{b_n}e^{-c_n} \qquad (81)
\end{aligned}$$

where

$$\begin{aligned}
a_n &= \left(\frac{(\phi_n + 1)\rho_r}{a_2\beta\rho_s(1 - \phi_n)\hat{\beta}_{s1}}\right)^k\sqrt{(1 - \phi_n^2)},\\
b_n &= 2a_2\beta + a_1(\phi_n + 1), \quad c_n = \left(\frac{(\phi_n + 1)\delta_4}{a_2\beta\rho_s(1 - \phi_n)\hat{\beta}_{s1}}\right),\\
p_n &= \left(\frac{(\phi_n + 1)\rho_r}{a_2\beta\rho_s(1 - \phi_n)\hat{\beta}_{s1}} + \frac{1}{k_1\hat{\beta}_{r1}}\right)^{-k-\hat{m}_{r1}},\\
\phi_n &= cos\left(\frac{(2n - 1)\pi}{2N}\right)
\end{aligned}$$

and N is the complexity-accuracy trade off parameter. Substituting (81) in (79) gives (37). Now, when $k_1 = 0$, $E[R_1^{FD}]$ can be determined by finding $F_{\Gamma_{11}}^{FD}(x)$ and substituting in (35). Accordingly,

$$\begin{aligned}
&F_{\Gamma_{11}}^{FD}(x)\\
&= 1 - P_r\left(\frac{|\hat{h}_{s1}|^2\rho_s a_1}{\beta a_2\rho_s|\hat{h}_{s1}|^2 + \delta_4} > x\right)\\
&= 1 - P_r\left(|\hat{h}_{s1}|^2 > \frac{x\delta_4}{\rho_s(a_1 - x\beta a_2)}\right) \qquad (82)\\
&= 1 - e^{-\frac{x\delta_4}{\rho_s(a_1 - xa_2\beta)\hat{\beta}_{s1}}}\sum_{k=0}^{\hat{m}_{s1}-1}\frac{1}{k!}\left(\frac{x\delta_4}{\rho_s(a_1 - xa_2\beta)\hat{\beta}_{s1}}\right)^k \qquad (83)
\end{aligned}$$

Substituting (83) in (35), $E[R_1^{FD}]$ is given by

$$E[R_1^{FD}] = \frac{1}{ln2}\sum_{k=0}^{\hat{m}_{s1}-1}\frac{1}{k!}\int_{x=0}^{\frac{a_1}{a_2\beta}}\frac{e^{-\frac{x\delta_4}{\rho_s(a_1-xa_2\beta)\hat{\beta}_{s1}}}}{1+x} \times\left(\frac{x\delta_4}{\rho_s(a_1-xa_2\beta)\hat{\beta}_{s1}}\right)^k dx \cong \frac{\pi}{Nln2}\sum_{k=0}^{\hat{m}_{s1}-1}\frac{1}{k!}\sum_{n=1}^{N}\frac{o_n}{b_n}e^{-c_n} \tag{84}$$

where $o_n = \left(\frac{(\phi_n+1)\delta_4}{a_2\beta\rho_s(1-\phi_n)\hat{\beta}_{s1}}\right)^k\sqrt{(1-\phi_n^2)}$. Thus the proposition 4 is proved.

APPENDIX E
DERIVATION OF (40) AND (41)

To determine $E[R_2^{FD}]$ using (39), we find the CDF of Y as follows:

$$\begin{aligned}F_Y(y) &= P_r\{\min(\Gamma_{12}^{FD},\Gamma_{r2}^{FD},\Gamma_{22}^{FD}\leq y)\}\\ &= 1-[P_r(\Gamma_{12}^{FD}>y)\times P_r(\Gamma_{r2}^{FD}>y)\times P_r(\Gamma_{22}^{FD}>y)]\\ &\triangleq 1-[A_1\times A_2\times A_3]\end{aligned} \tag{85}$$

Now A_1, A_2 and A_3 are determined as follows:

$$\begin{aligned}A_1 &= P_r(\Gamma_{12}^{FD}>y) = P_r\left(\frac{|\hat{h}_{s1}|^2\rho_s a_2}{|\hat{h}_{s1}|^2\rho_s a_1+|\hat{h}_{r1}|^2\rho_r+\delta_3}>y\right)\\ &= P_r\left(|\hat{h}_{s1}|^2 > \frac{y(|\hat{h}_{r1}|^2\rho_r+\delta_3)}{\rho_s(a_2-a_1y)}\right)\\ &= \frac{(k_1\hat{\beta}_{r1})^{-\hat{m}_{r1}}}{\Gamma(\hat{m}_{r1})}e^{-\frac{y\delta_3}{\rho_s(a_2-ya_1)\hat{\beta}_{s1}}}\sum_{j=0}^{\hat{m}_{s1}-1}\frac{1}{j!}\left(\frac{y\rho_r}{\rho_s(a_2-ya_1)\hat{\beta}_{s1}}\right)^j\\ &\quad\times\int_{z=0}^{\infty}e^{-\left(\frac{y\rho_r}{\rho_s(a_2-ya_1)\hat{\beta}_{s1}}+\frac{1}{k_1\hat{\beta}_{r1}}\right)z}(z\rho_r+\delta_3)^j z^{\hat{m}_{r1}-1}dz\end{aligned} \tag{86}$$

By using Binomial expansion, (86) can be written as,

$$\begin{aligned}A_1 &= 1-\Bigg[\frac{(k_1\hat{\beta}_{r1})^{-\hat{m}_{r1}}}{\Gamma(\hat{m}_{r1})}e^{-\frac{y\delta_3}{\rho_s(a_2-ya_1)\hat{\beta}_{s1}}}\sum_{j=0}^{\hat{m}_{s1}-1}\frac{1}{j!}\\ &\quad\times\left(\frac{y\rho_r}{\rho_s(a_2-ya_1)\hat{\beta}_{s1}}\right)^j\sum_{i=0}^{j}{}^jC_i\left(\frac{\delta_3}{\rho_r}\right)^{j-i}\\ &\quad\times\int_{z=0}^{\infty}e^{-\left(\frac{y\rho_r}{\rho_s(a_2-ya_1)\hat{\beta}_{s1}}+\frac{1}{k_1\hat{\beta}_{r1}}\right)z}z^{j+\hat{m}_{r1}-1}dz\Bigg]\end{aligned} \tag{87}$$

Using [42] (3.351.3), (87) can be written as

$$\begin{aligned}A_1 &= 1-\Bigg[\frac{(k_1\hat{\beta}_{r1})^{-\hat{m}_{r1}}}{\Gamma(\hat{m}_{r1})}e^{-\frac{y\delta_3}{\rho_s(a_2-ya_1)\hat{\beta}_{s1}}}\sum_{j=0}^{\hat{m}_{s1}-1}\frac{1}{j!}\\ &\quad\times\left(\frac{y\rho_r}{\rho_s(a_2-ya_1)\hat{\beta}_{s1}}\right)^j\\ &\quad\times\sum_{i=0}^{j}{}^jC_i\left(\frac{\delta_3}{\rho_r}\right)^{j-i}(i+\hat{m}_{r1}-1)!\\ &\quad\times\left(\frac{y\rho_r}{\rho_s(a_2-ya_1)\hat{\beta}_{s1}}+\frac{1}{k_1\hat{\beta}_{r1}}\right)^{-j-\hat{m}_{r1}}\Bigg]\end{aligned} \tag{88}$$

$$\begin{aligned}A_2 &= P_r(\Gamma_{r2}^{FD}>y) = P_r\left(\frac{|\hat{h}_{sr}|^2\rho_s a_2}{|\hat{h}_{sr}|^2\rho_s a_1+|h_{rr}|^2\rho_r+\delta_1}>y\right)\\ &= P_r\left\{|\hat{h}_{sr}|^2 > \frac{y(|h_{rr}|^2\rho_r+\delta_1)}{\rho_s(a_2-a_1y)}\right\}\end{aligned} \tag{89a}$$

Notice that (89a) is similar to the term X_0 defined in (63d). Thus A_2 can be obtained similar to X_0 given in (66) and is given by

$$\begin{aligned}A_2 &= e^{-\frac{\delta_1 y}{\rho_s(a_2-a_1y)\hat{\beta}_{sr}}}\frac{(k_2\beta_{rr})^{-m_{rr}}}{\Gamma(m_{rr})}\sum_{l=0}^{\hat{m}_{sr}-1}\frac{1}{l!}\\ &\quad\times\left(\frac{\rho_r y}{\rho_s(a_2-a_1y)\hat{\beta}_{sr}}\right)^l\sum_{k=0}^{l}{}^lC_k\left(\frac{\delta_1}{\rho_r}\right)^{l-k}(k+m_{rr}-1)!\\ &\quad\times\left(\frac{\rho_r y}{\rho_s(a_2-a_1y)\hat{\beta}_{sr}}+\frac{1}{k_2\beta_{rr}}\right)^{-k-m_{rr}}\end{aligned} \tag{89b}$$

Further, A_3 is similar to Y_0 in (63d) and (67); thus A_3 is given by

$$A_3 = e^{-\frac{y\delta_2}{\rho_r\hat{\beta}_{r2}}}\sum_{q=0}^{\hat{m}_{r2}-1}\frac{1}{q!}\left(\frac{y\delta_2}{\rho_r\hat{\beta}_{r2}}\right)^q \tag{90}$$

Substituting (86), (89b) and (90) in (85) gives $F_Y(y)$. Using $F_Y(y)$ in (39) and rearranging, $E[R_2^{FD}]$ becomes:

$$\begin{aligned}E[R_2^{FD}] &= \frac{(k_2\beta_{rr})^{-m_{rr}}}{\Gamma(m_{rr})}\sum_{j=0}^{\hat{m}_{s1}-1}\frac{1}{j!}\sum_{l=0}^{\hat{m}_{sr}-1}\frac{1}{l!}\sum_{k=0}^{l}{}^lC_k\left(\frac{\delta_1}{\rho_r}\right)^{l-k}\\ &\quad\times(m_{rr}+k-1)!\sum_{q=0}^{\hat{m}_{r2}-1}\frac{1}{q!}\frac{1}{ln2}\\ &\quad\times\int_0^{a_2/a_1}e^{-\frac{y\delta_1}{(a_2-a_1y)\rho_s\hat{\beta}_{sr}}}e^{-\frac{\delta_3 y}{\rho_s(a_2-a_1y)\hat{\beta}_{s1}}}\\ &\quad\times\left(\frac{\rho_r y}{\rho_s(a_2-a_1y)\hat{\beta}_{s1}}\right)^j\left(\frac{y\rho_r}{\rho_s(a_2-a_1y)\hat{\beta}_{sr}}\right)^l\\ &\quad\times\left(\frac{y\rho_r}{\rho_s(a_2-ya_1)\hat{\beta}_{s1}}+\frac{1}{k_1\hat{\beta}_{r1}}\right)^{-j-\hat{m}_{r1}}\\ &\quad\times\left(\frac{y\rho_r}{\rho_s(a_2-a_1y)\hat{\beta}_{sr}}+\frac{1}{\beta_{rr}k_2}\right)^{-m_{rr}-k}\\ &\quad\times e^{-\frac{\delta_2 y}{\rho_r\hat{\beta}_{r2}}}\left(\frac{\delta_2 y}{\rho_r\hat{\beta}_{r2}}\right)^q\frac{1}{1+y}dy\end{aligned} \tag{91}$$

Let the integral in (91) be represented as I_1. Since I_1 cannot be reduced to a closed-form expression, we use the Gaussian-Chebyshev quadrature [43] to find an approximation for I_1. By substituting $y = \frac{1}{2}\frac{a_2}{a_1}(1+\phi_n)$ and using (80), I_1 becomes,

$$I_1 \cong \frac{\pi}{N}\sum_{n=1}^{N}\frac{d_n e_n f_n g_n q_n}{r_n}e^{-s_n}e^{-t_n}e^{-v_n} \tag{92}$$

where

$$d_n = \left(\frac{a_2(\phi_n+1)\rho_r}{a_2(1-\phi_n)\rho_s\hat{\beta}_{s1}}\right)^j\sqrt{1-\phi_n^2},$$
$$e_n = \left(\frac{a_2(\phi_n+1)\rho_r}{a_2(1-\phi_n)\rho_s\hat{\beta}_{sr}}\right)^l,$$

$$f_n = \left(\frac{\rho_r a_2(1+\phi_n)}{a_2(1-\phi_n)\rho_s\hat{\beta}_{sr}} + \frac{1}{k_2\beta_{rr}}\right)^{-m_{rr}-k},$$
$$g_n = (\frac{\delta_2\, a_2(\phi_n+1)}{2\, a_1\rho_r\hat{\beta}_{r2}})^q,$$
$$q_n = \left(\frac{\rho_r a_2(1+\phi_n)}{a_2(1-\phi_n)\rho_s\hat{\beta}_{s1}} + \frac{1}{k_1\hat{\beta}_{r1}}\right)^{-\hat{m}_{r1}-j},$$
$$s_n = (\frac{a_2(\phi_n+1)\rho_r}{a_2(1-\phi_n)\rho_s\hat{\beta}_{sr}}),$$
$$t_n = (\frac{a_2(\phi_n+1)\delta_3}{a_2(1-\phi_n)\rho_s\hat{\beta}_{s1}}), \quad v_n = \frac{\delta_2\, a_2(\phi_n+1)}{2\, a_1\rho_r\hat{\beta}_{r2}},$$
$$r_n = \frac{2\, a_1 + a_2(\phi_n+1)}{2\, a_1}, \quad \phi_n = cos(\frac{(2n-1)\pi}{2N})$$

and N is the complexity-accuracy trade-off parameter [43]. Substituting (92) in (91) gives (40). Now, when $k_1 = 0$, A_1 can be obtained as:

$$\begin{aligned} A_1 &= P_r(\Gamma_{12} > y) \\ &= P_r\left(\frac{|\hat{h}_{s1}|^2\rho_s a_2}{|\hat{h}_{s1}|^2\rho_s a_1 + \delta_3} > y\right) \\ &= P_r\left(|\hat{h}_{s1}|^2 > \frac{\delta_3 y}{\rho_s(a_2 - a_1 y)}\right) \\ &= e^{-\frac{\delta_3 y}{\rho_s(a_2-a_1y)\hat{\beta}_{s1}}} \sum_{j=0}^{\hat{m}_{s1}-1} \frac{1}{j!}\left(\frac{\delta_3 y}{\rho_s(a_2-a_1y)\hat{\beta}_{s1}}\right)^j \end{aligned} \tag{93}$$

It can be seen that A_2 and A_3 are same as those expressions obtained earlier, i.e., (89b) and (90) respectively. Substituting A_1, A_2, A_3 in (85), we get modified expression for $F_Y(y)$ for the case of $k_1 = 0$. Utilizing $F_Y(y)$ in (39), the new expression for $E[R_2^{FD}]$ is obtained as:

$$\begin{aligned} E[R_2^{FD}] = &\frac{(k_2\beta_{rr})^{-m_{rr}}}{\Gamma(m_{rr})} \sum_{j=0}^{\hat{m}_{s1}-1}\frac{1}{j!}\sum_{l=0}^{\hat{m}_{sr}-1}\frac{1}{l!}\left(\frac{1}{\rho_r}\right)^l \sum_{k=0}^{l} {}^lC_k \\ &\times\left(\frac{\delta_1}{\rho_r}\right)^{l-k}(m_{rr}+k-1)! \sum_{q=0}^{\hat{m}_{r2}-1}\frac{1}{q!} \\ &\times\frac{1}{ln2}\int_0^{a_2/a_1} e^{-\frac{y\delta_1}{(a_2-a_1y)\rho_s\hat{\beta}_{sr}}} e^{-\frac{\delta_3 y}{\rho_s(a_2-a_1y)\hat{\beta}_{s1}}} \\ &\times\left(\frac{\delta_3 y}{\rho_s(a_2-a_1y)\hat{\beta}_{s1}}\right)^j\left(\frac{y\rho_r}{\rho_s(a_2-a_1y)\hat{\beta}_{sr}}\right)^l \\ &\times\left(\frac{y\rho_r}{\rho_s(a_2-a_1y)\hat{\beta}_{sr}} + \frac{1}{\beta_{rr}k_2}\right)^{-m_{rr}-k} \\ &\times e^{-\frac{\delta_2 y}{\rho_r\hat{\beta}_{r2}}}\left(\frac{\delta_2 y}{\rho_r\hat{\beta}_{r2}}\right)^q \frac{1}{1+y}dy \end{aligned} \tag{94}$$

Let the integral term in (94) be I_2. Using, the Gaussian-Chebyshev quadrature method [43], I_2 can be simplified as

$$I_2 \cong \frac{\pi}{N}\sum_{n=1}^{N}\frac{w_n e_n f_n g_n}{r_n} e^{-s_n}e^{-t_n}e^{-v_n} \tag{95}$$

where $w_n = (\frac{a_2(\phi_n+1)\delta_3}{a_2(1-\phi_n)\rho_s\hat{\beta}_{s1}})^j\sqrt{1-\phi_n^2}$. Further, $e_n, f_n, g_n, s_n, t_n, v_n, r_n, \phi_n$ and N are defined as above. Substituting (95) in (94) gives (41). Proposition 5 is thus proved.

REFERENCES

[1] S. M. R. Islam, N. Avazov, O. A. Dobre, and K.-S. Kwak, "Power-domain non-orthogonal multiple access (NOMA) in 5G systems: Potentials and challenges," *IEEE Commun. Surveys Tuts.*, vol. 19, no. 2, pp. 721–742, 2nd Quart., 2017.

[2] Z. Ding, X. Lei, G. K. Karagiannidis, R. Schober, J. Yuan, and V. Bhargava, "A survey on non-orthogonal multiple access for 5G networks: Research challenges and future trends," *IEEE J. Sel. Areas Commun.*, vol. 35, no. 10, pp. 2181–2195, Oct. 2017.

[3] Z. Ding, M. Peng, and H. V. Poor, "Cooperative non-orthogonal multiple access in 5G systems," *IEEE Commun. Lett.*, vol. 19, no. 8, pp. 1462–1465, Aug. 2015.

[4] J.-B. Kim and I.-H. Lee, "Non-orthogonal multiple access in coordinated direct and relay transmission," *IEEE Commun. Lett.*, vol. 19, no. 11, pp. 2037–2040, Nov. 2015.

[5] Z. Zhang, K. Long, A. V. Vasilakos, and L. Hanzo, "Full-duplex wireless communications: Challenges, solutions, and future research directions," *Proc. IEEE*, vol. 104, no. 7, pp. 1369–1409, Jul. 2016.

[6] G. Liu, F. R. Yu, H. Ji, V. C. M. Leung, and X. Li, "In-band full-duplex relaying: A survey, research issues and challenges," *IEEE Commun. Surveys Tuts.*, vol. 17, no. 2, pp. 500–524, 2nd Quart., 2015.

[7] J.-B. Kim and I.-H. Lee, "Capacity analysis of cooperative relaying systems using non-orthogonal multiple access," *IEEE Commun. Lett.*, vol. 19, no. 11, pp. 1949–1952, Nov. 2015.

[8] Y. Liu, Z. Ding, M. Elkashlan, and H. V. Poor, "Cooperative non-orthogonal multiple access with simultaneous wireless information and power transfer," *IEEE J. Sel. Areas Commun.*, vol. 34, no. 4, pp. 938–953, Apr. 2015.

[9] P. Xu, Z. Yang, Z. Ding, and Z. Zhang, "Optimal relay selection schemes for cooperative NOMA," *IEEE Trans. Veh. Technol.*, vol. 67, no. 8, pp. 7851–7855, Aug. 2018.

[10] J. Zhao, Z. Ding, P. Fan, Z. Yang, and G. K. Karagiannidis, "Dual relay selection for cooperative NOMA with distributed space time coding," *IEEE Access*, vol. 6, pp. 20440–20450, 2018.

[11] Y. Zhou, V. W. S. Wong, and R. Schober, "Dynamic decode-and-forward based cooperative NOMA with spatially random users," *IEEE Trans. Wireless Commun.*, vol. 17, no. 5, pp. 3340–3356, May 2018.

[12] M. F. Kader and S. Y. Shin, "Coordinated direct and relay transmission using uplink NOMA," *IEEE Wireless Commun. Lett.*, vol. 7, no. 3, pp. 400–403, Jun. 2018.

[13] Y. Guo, Y. Li, Y. Li, W. Cheng, and H. Zhang, "SWIPT assisted noma for coordinated direct and relay transmission," in *Proc. IEEE/CIC Int. Conf. Commun. China (ICCC)*, Beijing, China, Aug. 2018, pp. 111–115.

[14] Y. Xu, G. Wang, L. Zheng, and S. Jia, "Performance of NOMA-based coordinated direct and relay transmission using dynamic scheme," *IET Commun.*, vol. 12, no. 18, pp. 2231–2242, Nov. 2018.

[15] C. Zhong and Z. Zhang, "Non-orthogonal multiple access with cooperative full-duplex relaying," *IEEE Commun. Lett.*, vol. 20, no. 12, pp. 2478–2481, Dec. 2016.

[16] M. Vaezi, R. Schober, Z. Ding, and H. V. Poor, "Non-orthogonal multiple access: Common myths and critical questions," *IEEE Wireless Commun.*, vol. 26, no. 5, pp. 174–180, Oct. 2019.

[17] Y. Gao, B. Xia, Y. Liu, Y. Yao, K. Xiao, and G. Lu, "Analysis of the dynamic ordered decoding for uplink NOMA systems with imperfect CSI," *IEEE Trans. Veh. Technol.*, vol. 67, no. 7, pp. 6647–6651, Jul. 2018.

[18] T.-L. Nguyen and D.-T. Do, "Power allocation schemes for wireless powered NOMA systems with imperfect CSI: An application in multiple antenna-based relay," *Int. J. Commun. Syst.*, vol. 31, no. 15, p. 3789, 2018.

[19] X. Li, J. Li, P. T. Mathiopoulos, D. Zhang, L. Li, and J. Jin, "Joint impact of hardware impairments and imperfect CSI on cooperative SWIPT NOMA multi-relaying systems," in *Proc. IEEE/CIC Int. Conf. Commun. China (ICCC)*, China, Aug. 2018, pp. 95–99.

[20] M. R. Zamani, M. Eslami, M. Khorramizadeh, and Z. Ding, "Energy-efficient power allocation for NOMA with imperfect CSI," *IEEE Trans. Veh. Technol.*, vol. 68, no. 1, pp. 1009–1013, Jan. 2019.

[21] L. Dai, B. Wang, Z. Ding, Z. Wang, S. Chen, and L. Hanzo, "A survey of non-orthogonal multiple access for 5G," *IEEE Commun. Surveys Tuts.*, vol. 20, no. 3, pp. 2294–2323, 3rd Quart., 2018.

[22] C. Wang, T. C.-K. Liu, and X. Dong, "Impact of channel estimation error on the performance of amplify-and-forward two-way relaying," *IEEE Trans. Veh. Technol.*, vol. 61, no. 3, pp. 1197–1207, Mar. 2012.

[23] X. Yue, Y. Liu, S. Kang, A. Nallanathan, and Z. Ding, "Exploiting full/half-duplex user relaying in NOMA systems," *IEEE Trans. Commun.*, vol. 66, no. 2, pp. 560–575, Feb. 2017.
[24] C. Guo, L. Zhao, C. Feng, Z. Ding, and H.-H. Chen, "Energy harvesting enabled NOMA systems with full-duplex relaying," *IEEE Trans. Veh. Technol.*, vol. 68, no. 7, pp. 7179–7183, Jul. 2019.
[25] L. Zhang, J. Liu, M. Xiao, G. Wu, Y.-C. Liang, and S. Li, "Performance analysis and optimization in downlink NOMA systems with cooperative full-duplex relaying," *IEEE J. Sel. Areas Commun.*, vol. 35, no. 10, pp. 2398–2412, Oct. 2017.
[26] T. M. C. Chu and H.-J. Zepernick, "Performance of a non-orthogonal multiple access system with full-duplex relaying," *IEEE Commun. Lett.*, vol. 22, no. 10, pp. 2084–2087, Oct. 2018.
[27] O. Abbasi and A. Ebrahimi, "Cooperative NOMA with full-duplex amplify- and-forward relaying," *Trans. Emerg. Telecommun. Technol.*, vol. 29, no. 7, p. e3421, Jul. 2018.
[28] T. E. A. Alharbi and D. K. C. So, "Full-duplex decode-and-forward cooperative non-orthogonal multiple Access," in *Proc. IEEE 87th Veh. Technol. Conf. (VTC Spring)*, Porto, Portugal, Jun. 2018, pp. 1–6.
[29] N. T. Tan, T. M. Hoang, B. C. Nguyen, and L. T. Dung, "Outage analysis of downlink NOMA full-duplex relay networks with RF energy harvesting over Nakagami-m fading channel," in *Proc. Int. Conf. Eng. Res. Appl.*, Nov. 2018, pp. 477–487.
[30] M. B. Shahab and S. Y. Shin, "Time shared half/full-duplex cooperative NOMA with clustered cell edge users," *IEEE Wireless Commun. Lett.*, vol. 22, no. 9, pp. 1794–1797, Sep. 2018.
[31] T.-T.-H. Nguyen and X.-N. Tran, "Performance of cooperative NOMA system with a full-duplex relay over Nakagami-m fading channels," in *Proc. 3rd Int. Conf. Recent Adv. Signal Process. Telecommun. Comput. (SigTelCom)*, Mar. 2019, pp. 130–134.
[32] X. Li, M. Liu, C. Deng, P. T. Mathiopoulos, Z. Ding, and Y. Liu, "Full-duplex cooperative NOMA relaying Systems with I/Q imbalance and imperfect SIC," *IEEE Wireless Commun. Lett.*, to be published.
[33] X.-X. Nguyen and D.-T. Do, "System performance of cooperative NOMA with full-duplex relay over Nakagami-m fading channels," *Mobile Inf. Syst.*, vol. 2019, Mar. 2019, Art. no. 7547431.
[34] X. Li and L. Meng, "Joint effects of residual hardware impairments and channel estimation errors on SWIPT assisted cooperative NOMA networks," *IEEE Access*, vol. 7, pp. 135499–135513, 2019.
[35] X. Li, J. Li, and L. Li, "Performance Analysis of Impaired SWIPT NOMA Relaying Networks over Imperfect Weibull Channels," *IEEE Syst. J.*, to be published.
[36] A. Goldsmith, *Wireless Communications*, Cambridge, U.K.: Cambridge Univ. Press, 2005.
[37] E. Everett, M. Duarte, C. Dick, and A. Sabharwal, "Empowering full-duplex wireless communication by exploiting directional diversity," in *Proc. Conf. Rec. 45th Asilomar Conf. Signals Syst. Comput. (ASILOMAR)*, Pacific Grove, CA, USA, Nov. 2011, pp. 2002–2006.
[38] M. A. Khojastepour, K. Sundaresan, S. Rangarajan, X. Zhang, and S. Barghi, "The case for antenna cancellation for scalable full-duplex wireless communications," in *Proc. 10th Workshop Hot Topics Netw.*, 2017, p. 17.
[39] T. Riihonen, S. Werner, and R. Wichman, "Mitigation of loopback self-interference in full-duplex MIMO relays," *IEEE Trans. Signal Process.*, vol. 59, no. 12, pp. 5983–5993, Dec. 2011.
[40] E. Everett, A. Sahai, and A. Sabharwal, "Passive self-interference suppression for full-duplex infrastructure nodes," *IEEE Trans. Wireless Commun.*, vol. 13, no. 2, pp. 680–694, Jan. 2014.
[41] M. Duarte, C. Dick, and A. Sabharwal, "Experiment-driven characterization of full-duplex wireless systems," *IEEE Trans. Wireless Commun.*, vol. 11, no. 12, pp. 4296–4307, Dec. 2012.
[42] I. S. Gradshteyn and I. M. Ryzhik, *Table of Integrals, Series and Products*, 7th ed. New York, NY, USA: Academic, 2007.
[43] E. Hildebrand, *Introduction to Numerical Analysis*. New York, NY, USA: Dover, 1987.

V. ASWATHI received the B.Tech. degree in electronics and communication engineering and the M.Tech. degree in communication engineering and signal processing from Calicut University, in 2016. She is currently pursuing the Ph.D. degree with the Electronics and Communication Department, National Institute of Technology, Calicut. Her current research interest includes non-orthogonal multiple access-based 5G networks.

A. V. BABU received the M.E. degree in telecommunication from the Department of Electrical Communication Engineering, Indian Institute of Science, Bengaluru, India, in 2002, and the Ph.D. degree from the Department of Electronics and Communication Engineering, National Institute of Technology, Calicut, India, in 2008. He is currently a Professor with the Department of Electronics and Communication Engineering, National Institute of Technology. He has authored or coauthored more than 75 articles in reputed international journals and conferences. His primary research focus is on wireless networks and the current research interest includes resource allocation for NOMA-based 5G wireless networks.